

MORPHOMETRIC AND MORPHOLOGICAL-BASED  
NONINVASIVE SEX IDENTIFICATION OF BLOOD  
COCKLE, *Tegillarca granosa* (LINNAEUS, 1758)

A Special Problem

Presented to

the Faculty of the Division of Physical Sciences and Mathematics

College of Arts and Sciences

University of the Philippines Visayas

Miag-ao, Iloilo

In Partial Fulfillment

of the Requirements for the Degree of

Bachelor of Science in Computer Science by

ADRICULA, Briana Jade

PAJARILLA, Gliezel Ann

VITO, Ma. Christina Kane

Francis DIMZON, Ph.D.

Adviser

Victor Marco Emmanuel FERRIOLS, Ph.D.

Co-Adviser

June 2025

**Approval Sheet**

The Division of Physical Sciences and Mathematics, College of Arts and Sciences, University of the Philippines Visayas

certifies that this is the approved version of the following special problem:

**MORPHOMETRIC AND MORPHOLOGICAL-BASED  
NONINVASIVE SEX IDENTIFICATION OF BLOOD  
COCKLE, *Tegillarca granosa* (LINNAEUS, 1758)**

**Approved by:**

Name	Signature	Date
Francis D. Dimzon, Ph.D. (Adviser)	_____	_____
Victor Marco Emmanuel N. Ferriols, Ph.D. (Co-Adviser)	_____	_____
Ara Abigail E. Ambita (Panel Member)	_____	_____
Kent Christian A. Castor (Division Chair)	_____	_____

Division of Physical Sciences and Mathematics

College of Arts and Sciences

University of the Philippines Visayas

**Declaration**

We, Briana Jade Adricula, Gliezel Ann Pajarilla, and Ma. Christina Kane Vito, hereby certify that this Special Problem has been written by us and is the record of work carried out by us. Any significant borrowings have been properly acknowledged and referred.

**Name**

**Signature**

**Date**

Briana Jade D. Adricula

\_\_\_\_\_

(Student)

Gliezel Ann T. Pajarilla

\_\_\_\_\_

(Student)

Ma. Christina Kane B. Vito

\_\_\_\_\_

(Student)

## Dedication

**To our family, advisers, and the people of science:**

A heart full of love,

To those who gave wings so we can fly.

Stood firm even through moments of doubt.

A jovial harmony and warmth that kept us steadfast.

A word of thanks is an understatement,

To those who cast their light upon our way.

A source of wisdom even when the road grew heavy,

A north star that guided us through this journey.

Immeasurable esteem we offer,

To the unsung heroes of science and innovation,

Whose drive and dedication uplift and inspire,

Changing lives with boundless determination.

## Acknowledgment

### I. General Acknowledgment

The researchers would like to extend their heartfelt gratitude to the significant people who were part of this journey. These people extended their expertise, support, and guidance, which made this whole process bearable and fulfilling.

First and foremost, to the Almighty God who gives us the strength to never lose hope throughout the challenging moments in our journey; for the wisdom and perseverance He bestowed upon us to accomplish this paper. All for His unconditional love, mercy, and grace. All glory and praise to Him.

To our research adviser who provided guidance and support to the researchers, and for the help when things were hard. Dr. Francis Dimzon – thank you for guiding us throughout this journey. We would like to thank you for assuring us, especially when we were about to turn around halfway. We would like to extend our greatest gratitude for the consistent supervision by providing us with valuable feedback and insightful comments that aided us in our methodology and in completing this paper.

To our co-adviser who was willing to tour us around the hatchery facility and helped us come up with this study. Thank you, Dr. Victor Marco Emmanuel Ferriols, for sharing your knowledge and wisdom with us researchers. Thank you for answering our questions and extending your time with us. Additionally, the most important part of the research is the samples — the blood cockle samples — thank you for providing them willingly. You served as an inspiration for us to apply solutions to real-world problems, especially in aquaculture.

To the research associates and hatchery staff of the UPV Hatchery, Ms. Allena Arteta, Ms. LC May Gasit, Ms. Shiela Untalan, and the hatchery staff, Mr. Paul Andre Lopez and Mr. Joel M. Fabrigas, for assisting us in handling the blood cockles, teaching us how to identify their sex, spawning, and dissection. A big thanks to Ms. Allena Arteta for letting us borrow the camera stand that we used in the entire data gathering process. Your constant warmth and assistance went beyond learning the basics; instead, we learned a whole lot more, especially the importance of creating solutions for aquaculture practices.

Lastly, to everyone who directly or indirectly contributed to this thesis, whether through words of encouragement, technical advice, or simply by believing in us, we offer our sincerest gratitude. This study would also not have been possible without you.

### i. Adricula's Acknowledgment

I would like to express my deepest gratitude to my beloved family who supported me throughout my academic journey. My Mama Madelene and Papa Juvy, who have made countless sacrifices to make me the person I am today. To my sister, Aianna, and cousins Jayson, Joana, and Joel, who have helped me unwind after long and stressful days of academic load. To my aunt, Tita Lybel – thank you for believing in me since day one. You are always there to guide me in every decision I make. And to my Lola Lydia, who has been my inspiration in finishing my studies. Your reminders to eat more and stay safe have always kept me grounded and cared for, and I appreciate the extra allowance you always give me whenever I go back to Miagao. Without such a supportive family behind me, I

couldn't have done this without you.

To my pretty college friends, Arianne, Gliezel, Karielle, Kane, Kzlyr, and Sharah, thank you for making my college experience bearable. The laughter and joy that we shared together lessened the stress I felt. Here's to all the rants, tsismis, and bangs memories we had — look how far we've come. I will forever cherish the memories we made together through ups and downs. Thank you for the encouragement along the way and just for being there by my side.

To my co-researchers, Gliezel and Kane, this would not have been possible without you. Your insights and passion for this research inspired me along the way. Thank you for the teamwork, initiatives, and hard work. I will miss the dorm to hatchery to computer lab to dorm adventures with you!

To my second home, UPV Balay Gumamela, our dorm manager, and all the staff — thank you for checking up on me, always making me feel welcome, and ensuring that we had a comfortable stay.

And lastly, to the people who believed in me and have always been there for me every step of the way, even when life was harsh — I am forever grateful for your unwavering encouragement, support, and just for believing that I can make things possible.

## **ii. Pajarilla's Acknowledgment**

To my mother in heaven, Mama Eva, I made it through the last chapter of this paper. I felt your boundless love and support every step of the way. You will always be my source of strength and inspiration, even when hope seemed bleak

and weary. The different storms that were pushed my way — I stood because I know you believed in me and wanted the best for me and my three siblings.

Greatest love and appreciation to my siblings – my source of boundless joy. Your smiles, laughter, and warmth gave me a boost of energy that adenosine triphosphate can't surpass. Gil Ivan, Gillian Gella, and my small baby brother Gian Godric – no words can express how thankful I am for your existence and love, as it sparked perseverance and grit in my heart. To the people who cared and looked after me, thank you, Tito Rem and Auntie Maricel, for the financial support and encouragement. Thank you for believing in me and the things that I can achieve.

My heart is full of gratitude and appreciation to the Gumamela Girls Dormers. I cherish all the laughter, joy, sadness, ennui, anger, fear, embarrassment, anxiety, envy, and disgust. Kidding aside, I am forever thankful for the bond and friendship we made, the spontaneous moments, and baybay sessions, admiring the beauty of nature. Arianne, Briana, Kane, Karielle, Kzlyr, Sharah – thank you for the words of encouragement, for listening, and for your companionship.

I would like to extend my greatest appreciation to my co-researchers, Kane and Briana, who trailed the 100 steps from and to the hatchery facility. I appreciate the moments and laughter that we spent together, from ideation, spending almost the whole day in the computer laboratory to train our model, to crafting this final paper. We went through doubts and a series of burnout moments, but your presence made everything lighter.

My love and appreciation are offered to my high school and Senior High School friends who listened to my “I can't do this anymore” moments. Thank you,

Jara, Francine, Nellen, Mary, and Nyle, for cheering me on and believing in my potential, even when things sometimes got so dim. Thank you for reminding me that there is always light at the end of the tunnel. You all are my support system, cheering squad, and parents I met along the way.

My greatest thanks are relayed to Manang Myrtle, who offered kind words, warmth, and guidance. Thank you so much for the support, for offering your shoulders when I needed someone to rely on. Things felt a bit lighter with your smile and your “You can do it, Gliez.” Thank you so much for being my guardian for a year.

My gratitude extends to the people inside the university who served as family. To Ma’am Marites Geonanga, Ma’am Paula Khryss Ushiyama, Balay Gumamela dorm manager, Ma’am Celina Sumalapao and the dorm staff, Tita Ope, Tita Vilma, Nong Joefil, and the UPV Virgils — thank you for the support, for believing in me, and for the nutritional food that helped me brainstorm, conduct, and write this study.

To everyone who supported me, thank you so much. Words can’t express how grateful I am.

### **iii. Vito’s Acknowledgment**

To my beloved family – Mama, Papa, Mommy, Lola Jo, Uncle Mike, Tita Emie, Lola Shirley, and Lola Terry – thank you for your unconditional love, patience, and never-ending encouragement. Your strength and support have been the backbone of everything I’ve achieved. Your belief in me has always kept me grounded and

motivated, even when I doubted myself. Thank you for the constant prayers, thoughtful check-ins, and warm words that lifted me during the hardest times. Your financial support has also played an instrumental role in helping me pursue this journey, and I am deeply grateful.

To my lovely (but sometimes annoying) siblings – Hariette, Vladimir, Michaela, Regina, and Daniel – words can't fully express how much you mean to me. Thank you for being my constant source of joy, laughter, and sanity. Through all the sibling chaos, inside jokes, and heart-to-heart conversations, you've kept me connected to the things that truly matter. Whether it was a random meme shared to make me laugh, a quick call just to check in, or simply being there in quiet support, you all reminded me that no matter where I was, I was never truly alone.

To my ever-reliable and ever-beautiful Gumamela Girls – Briana, Gliezel, Ari-anne, Sharah, Kai, and Kzlyr – thank you for the love, the chika, and the comfort. You all made even the most stressful days feel manageable. You've truly been my home away from home. Special mention to Briana and Gliezel, my fellow re-searchers, who stood by me not only as friends but as teammates navigating this academic journey together. Your dedication, the leg-torturing stairs we climbed to the hatchery for data gathering, and late-night grind sessions will always be one of my favorite parts of this experience.

To the UPV Virgils, thank you for being the silent heroes behind my survival. Your monthly grocery supplies kept me fed, sane, and functioning. I probably owe half of this thesis to the snacks.

To the Balay Gumamela dorm staff, thank you for being my guardians during my stay at the dorm. Your support, care, and constant presence made my time

away from home more comfortable and secure. I will always be grateful for the way you looked out for me and made me feel safe.

To my very cutesy, very demure, very mindful pet dogs, Chewy and Max – thank you for the joy and companionship you've brought into my life. Max, though you are no longer with us, your memory continues to live on in my heart. Chewy, thank you for being my ever-present companion, sharing both the quiet, loud, and the playful moments.

To chonky cat Mother Litob, your cuteness and presence in the hatchery during our data gathering made the 100-step stairs bearable. My tiredness would instantly vanish whenever I petted you.

This journey has been a collective effort – held up by the love, wisdom, laughter, and resilience of those around me. I am endlessly grateful for each of you.

## Abstract

*Tegillarca granosa*, commonly known as blood cockles, is a significant marine bivalve species due to its nutritional value and economic importance. Accurate sex identification is crucial for maintaining a balanced male-to-female ratio, supporting sustainable harvesting, and improving resource management. However, macroscopically identifying sex through shell morphology is challenging, and there are currently no available technologies for non-invasive sex classification. This study explores the use of machine learning and deep learning techniques to classify the sex of blood cockles based on shell measurements (length, width, height, hinge line length, distance between the umbos, and rib count) and images taken from various angles (dorsal, ventral, anterior, posterior, and lateral views). Machine learning analysis using k-nearest neighbors (KNN) achieved 64.16% accuracy, 64.97% precision, 64.16% recall, 63.75% F1 Score, and 70.04% area under the curve (AUC) score. Moreover, deep learning using convolutional neural networks (CNN) achieved 71.68% accuracy, 72.52% precision, 69.29% recall, 69.12% F1 Score, and 77.34% AUC score using images captured from the left lateral angle view. These results demonstrate the potential of a non-invasive approach to sex identification, supporting sustainable aquaculture practices and offering a baseline for further research using computer vision, machine learning, and deep learning.

**Keywords:** deep learning, supervised machine learning, computer vision, convolutional neural network, blood cockle, sex identification, *Tegillarca granosa*

# Contents

<b>1</b>	<b>Introduction</b>	<b>1</b>
1.1	Overview . . . . .	1
1.2	Problem Statement . . . . .	2
1.3	Research Objectives . . . . .	4
1.3.1	General Objective . . . . .	4
1.3.2	Specific Objectives . . . . .	4
1.4	Scope and Limitations of the Research . . . . .	5
1.5	Significance of the Research . . . . .	6
<b>2</b>	<b>Review of Related Literature</b>	<b>9</b>
2.1	Background on <i>T. granosa</i> and Their Importance . . . . .	10
2.2	Sex Identification Methods in <i>T. granosa</i> . . . . .	14

2.3	Machine Learning and Deep Learning in Biology . . . . .	17
2.3.1	Deep Learning for Phenotype Classification in Ark Shells .	17
2.3.2	Geometric Morphometrics and Machine Learning for Species Delimitation . . . . .	18
2.3.3	Contour Analysis in Mollusc Shells Using Machine Learning	18
2.3.4	Machine Learning for Shape Analysis of Marine Organisms	19
2.3.5	Deep Learning for Landmark-Free Morphological Feature Extraction . . . . .	21
2.3.6	Machine Learning for Sex Differentiation in Abalone . . .	22
2.3.7	Machine Learning for Geographical Traceability in Bivalves	23
2.4	Limitations on Sex Identification in <i>T. granosa</i> . . . . .	24
2.5	Chapter Summary . . . . .	26
<b>3</b>	<b>Research Methodology</b>	<b>29</b>
3.1	Sample Collection . . . . .	30
3.2	Ethical Considerations . . . . .	31
3.3	Creating <i>T. granosa</i> Dataset . . . . .	32
3.4	Morphometric Data Collection . . . . .	33
3.5	Image Acquisition and Data Gathering . . . . .	34

<b>CONTENTS</b>	xv
3.6    Hardware and Software Configuration . . . . .	35
3.7    Machine Learning on Morphometric Data . . . . .	36
3.7.1    Data Preprocessing . . . . .	36
3.7.2    Machine Learning Models Training . . . . .	38
3.8    Deep Learning for Morphological Analysis . . . . .	40
3.8.1    Image Preprocessing . . . . .	40
3.8.2    Convolutional Neural Network . . . . .	42
3.8.3    CNN Training . . . . .	44
3.9    Evaluation Metrics . . . . .	47
<b>4    Results and Discussions</b>	<b>51</b>
4.1    Machine Learning Analysis . . . . .	51
4.1.1    Data Exploration . . . . .	52
4.1.2    Statistical Analysis . . . . .	53
4.1.3    Feature Importance Analysis . . . . .	55
4.1.4    Performance Evaluation . . . . .	56
4.1.5    Visualizations for Machine Learning . . . . .	58
4.2    Deep Learning Analysis . . . . .	60

4.2.1	Baseline Model . . . . .	61
4.2.2	Comparison of Individual and Combined Angles . . . . .	62
4.2.3	Training Result and Hyperparameter Tuning . . . . .	63
4.2.4	Proposed Model . . . . .	64
4.2.5	Learning Rates and Training Behavior per Fold . . . . .	65
4.2.6	Visualizations for Deep Learning . . . . .	66
4.3	Discussions . . . . .	72
<b>5</b>	<b>Conclusion and Recommendations</b>	<b>75</b>
5.1	Conclusion . . . . .	75
5.2	Recommendations . . . . .	76
<b>6</b>	<b>References</b>	<b>79</b>
<b>A</b>	<b>Code Snippets</b>	<b>87</b>
<b>B</b>	<b>Resource Persons</b>	<b>93</b>
<b>C</b>	<b>Data Gathering Documentation</b>	<b>95</b>

# List of Figures

2.1	Diagram of <i>T. granosa</i> 's external anatomy. . . . .	12
3.1	Female <i>T. granosa</i> shells. . . . .	31
3.2	Male <i>T. granosa</i> shells. . . . .	31
3.3	Different views of the <i>T. granosa</i> shell captured. . . . .	32
3.4	Linear measurements that were gathered from the shell of <i>T. granosa</i> . .	34
3.5	Image acquisition setup for <i>T. granosa</i> samples. . . . .	35
3.6	Data preprocessing in machine learning pipeline. . . . .	36
3.7	Diagram of k-fold cross-validation with $k = 5$ . . . . .	39
3.8	Shadows removed from male samples at different angles. . . . .	41
3.9	Shadows removed from female samples at different angles. . . . .	41
3.10	Architecture of convolutional neural network (CNN). . . . .	42
3.11	Diagram of stratified k-fold cross-validation with $k=5$ . . . . .	45

3.12 On-the-Fly dataset augmentation (OnDAT) techniques. . . . .	46
4.1 Heatmap of morphometric correlations with <i>T. granosa</i> sex. . . . .	52
4.2 Feature importance scores using the Kruskal-Wallis test. . . . .	56
4.3 KNN confusion matrix for <i>T. granosa</i> sex classification. . . . .	59
4.4 ROC curve with AUC score for KNN. . . . .	60
4.5 Training and validation accuracy per fold. . . . .	67
4.6 Average training and validation accuracy across folds. . . . .	68
4.7 Training and validation loss per fold. . . . .	68
4.8 Average training and validation loss across folds. . . . .	69
4.9 Confusion matrix for CNN model (Batch Size: 32, Epochs: 50, Activation Function: ReLU). . . . .	70
4.10 ROC curve with area under the curve (AUC) score for the proposed model. . . . .	71
A.1 Feature engineering used to create and transform the dataset for machine learning analysis. . . . .	87
A.2 Feature importance scores derived from the Kruskal-Wallis test to identify the most significant variables. . . . .	88

A.3 Random undersampling applied in machine learning to address class imbalance. . . . .	88
A.4 Five-fold cross-validation used to evaluate and tune machine learning model performance. . . . .	89
A.5 Resizing images to 256x256 pixels for consistent input dimensions. . . . .	89
A.6 Processing the images to remove the shadows. . . . .	90
A.7 Random undersampling applied in deep learning to balance class distribution in the datasets. . . . .	91
A.8 On-the-fly data augmentation used to create a variety of random transformation to increase variation in the training images. . . . .	92
A.9 CNN architecture used for training the image dataset. . . . .	92
A.10 Early Stopping and ReduceLROnPlateau used as safeguard against overfitting. . . . .	92
C.1 Sex identification through spawning of <i>T. granosa</i> . . . . .	95
C.2 Sex-based separation of <i>T. granosa</i> samples post-spawning. . . . .	96
C.3 Sex identified female through dissection of <i>T. granosa</i> . . . . .	96
C.4 Sex identified male through dissection of <i>T. granosa</i> . . . . .	96
C.5 Linear measurements of female <i>T. granosa</i> . . . . .	97
C.6 Linear measurements of male <i>T. granosa</i> . . . . .	97

C.7	Captured images of female <i>T. granosa</i> . . . . .	98
C.8	Captured images of male <i>T. granosa</i> . . . . .	98

## List of Tables

2.1	Comparison of the methods used in bivalves studies. . . . .	27
3.1	Architecture of the convolutional neural network used. . . . .	44
4.1	Comparison of morphometric features between male and female <i>T. granosa</i> , showing mean and standard deviation (SD) values. . . . .	54
4.2	Mann-Whitney U test results for sex-based feature comparison. . . . .	55
4.3	Performance metrics for models with all 13 features. . . . .	57
4.4	Performance metrics for models with 5 features. . . . .	57
4.5	Performance metrics for balanced vs imbalanced datasets (Batch Size: 16, Epochs: 20). . . . .	61
4.6	Performance metrics for individual and combined angles (Batch Size: 16, Epochs: 20). . . . .	62
4.7	Effect of batch size and epoch values on CNN model performance. . . . .	64

4.8 Performance metrics for different activation functions (Batch Size: 32, Epochs: 50) . . . . .	64
4.9 Per-fold performance metrics (Batch Size: 32, Epochs: 50, Ac- tivation Function: ReLU) and corresponding mean and standard deviation. . . . .	65
4.10 Learning rate reductions, early stopping, and best epochs per fold during 5-fold cross-validation. . . . .	66

# Chapter 1

## Introduction

### 1.1 Overview

The Philippines is a global center of marine biodiversity and has established aquaculture as a significant contributor to total fishery production (Aypa & Bacongus, 2000; BFAR, 2019). The country produces over 4 million tonnes of seafood annually and is the 11th largest seafood producer in the world. Aquaculture is deeply integrated into Filipinos' livelihoods, encompassing fish cultivation and the production of various aquatic species, including bivalves. Among these, blood cockles (*Tegillarca granosa*) hold considerable economic and environmental significance, making it essential to ensure sustainable production and population balance.

Maintaining a balanced male-to-female ratio of blood cockles is crucial to prevent overharvesting and ensure sustainability. An imbalanced ratio can lead to over-exploitation and negatively impact the population's viability. However, there is limited literature on *T. granosa* that provides a thorough understanding of its

sex-determining mechanisms, particularly regarding sexual dimorphism based on morphometric and morphological characteristics (Breton, Capt, Guerra, & Stewart, 2017).

Currently, sex determination methods for blood cockles are invasive, including dissection and histological examinations, which often result in the death of the species. While there is growing literature on sex identification in aquaculture commodities using machine learning and deep learning, there remains a notable scarcity of research specific to *T. granosa* (Miranda & Ferriols, 2023).

This study aims to provide a detailed baseline analysis of blood cockles by leveraging their morphometric and morphological characteristics. Sexual dimorphism in bivalves is often subtle and challenging to establish macroscopically (Karapunar, Werner, Fürsich, & Nützel, 2021). However, by integrating machine learning and deep learning approaches, this study seeks to identify distinct traits that may differentiate male and female blood cockles.

## 1.2 Problem Statement

Identifying the sex of *Tegillarca granosa* is important for promoting sustainable aquaculture and biodiversity by maintaining a balanced male-to-female ratio. A balanced ratio helps prevent overharvesting. Although sex identification is crucial for blood cockle population management and sustainable aquaculture, there is a notable lack of research on creating noninvasive methods for determining the sex of *T. granosa*. Many recent studies and approaches rely on invasive methods like dissection or histological analysis, which are impractical for large-scale aquaculture

operations focused on conservation.

Current methods for determining the sex of *T. granosa* are invasive and involve dissection, which requires cutting open the shell to visually inspect the gonads (Erica, 2018). This procedure can cause harm to the specimens and frequently leads to their death. Another method is histological examination, where tissue samples are analyzed under a microscope (May, Maung, Phy, & Tun, 2021). Both approaches are labor-intensive and time-consuming, and can pose risks to population management, particularly when maintaining a balanced sex ratio for breeding programs is essential. Moreover, these invasive methods require specialized technical skills for accurate execution. Resource-limited aquaculture operations face significant challenges in accessing the necessary laboratory equipment, such as microscopes and staining tools, complicating the process.

A less invasive approach employed by aquaculturists involves monitor spawning behavior, where individuals are separated and stimulated to reproduce in order to determine their sex through the release of gametes (Miranda & Ferriols, 2023). Although this method is indeed less invasive than dissection, it still induces stress in blood cockles and may not be completely effective for fast identification in large populations.

Given the limitations of both invasive and less invasive methods, there is a clear need for a more advanced approach. An alternative, noninvasive method involving machine and deep learning technologies could address these issues by providing a fast, accurate, and effective solution without harming or stressing the blood cockles.

## 1.3 Research Objectives

### 1.3.1 General Objective

The general objective of this study is to develop a noninvasive method for identifying the sex of *Tegillarca granosa* using machine learning and deep learning technologies. This method aims to provide accurate and streamlined sex identification without causing harm to the specimens, thus supporting sustainable aquaculture practices.

### 1.3.2 Specific Objectives

To achieve the overall general objective of developing a noninvasive sex identification of *T. granosa* using machine learning and deep learning technologies, the following specific objectives have been established:

1. to collect and organize a comprehensive dataset of *T. granosa*, which will include linear measurements and images captured from different camera angles that will serve as the basis for training and evaluating the machine learning and deep learning models,
2. to develop and implement machine learning and deep learning models that can classify the sex of *T. granosa* based on the collected linear measurements and images of different camera angles of the sample, and determine the best performing models, and
3. to evaluate the model using performance metrics such as accuracy, preci-

sion, recall, F1 Score, and the area under the receiver operating characteristic curve (AUC-ROC) score, and improve it by performing hyperparameter optimization.

## 1.4 Scope and Limitations of the Research

This study is conducted alongside the ongoing research by the UPV DOST-PCAARRD, titled “Establishment of the Center for Mollusc Research and Development: Development of Spawning and Hatchery Techniques for the Blood Cockle (*Anadara granosa*) for Sustainable Aquaculture.” The ongoing research primarily involves the rearing of *Tegillarca granosa* from spat to larvae, feeding experiments, stocking density evaluations, substrate selection, and settlement rate assessments.

In contrast, this study mainly focused on developing a noninvasive method for identifying the sex of *T. granosa* using machine learning and deep learning technologies. The goal is to provide an accurate and efficient means of sex identification without causing harm to the samples, contributing to sustainable aquaculture practices.

The researchers worked with 271 blood cockles that had been sex-identified and taken from Panay Island, specifically sourced from Zarraga Iloilo and Ivisan Capiz. These samples, divided between 144 males and 127 females, were obtained through induced spawning via temperature shock and dissection. Data collection was limited to the spawned stage among the five gonadal stages - immature, developing, mature, spawning, and spent stages. The other stages were not preferable due to indistinguishable gonads and their inability to undergo induced spawning (May

et al., 2021). Thus, the researchers only focused on the samples undergoing the spawned stage.

During the data collection, the researchers personally gathered linear measurements, including length, width, height, rib count, hinge line length, and distance between the umbos through the vernier caliper. The data gathering process was supervised by the University Research Associates from the Institute of Aquaculture, College of Fisheries and Ocean Sciences. Aside from linear measurements, images were taken from six different angles. The process of linear measurements and image collection were noninvasive, considering the blood cockle-built ability to survive in low oxygen environments and naturally inhabit intertidal mudflats (Zhan & Bao, 2022).

The method developed in this study is specific to *T. granosa* and may not apply to other bivalve species. The model was trained exclusively for *T. granosa*'s morphometric and morphological features, which may not be consistent and applicable across other shellfish species.

## 1.5 Significance of the Research

This study will give us a significant advancement in noninvasive sex identification methods in *Tegillarca granosa*, providing innovative solutions that has the potential to address the challenges in identifying sex and reshape sustainable approaches to aquaculture. The significance of this study extends to the following:

*Research Institution.* The result of this study focusing on the sex-identification mechanism of bivalves, specifically *T. granosa*, will provide valuable insights into

universities and research centers that focus on fisheries and coastal management, such as the UPV Institute of Aquaculture, that aim to develop sustainable development and suitable culture techniques.

*Fisherfolks.* By developing a noninvasive method in sex identification, this study can help long-term harvest efficiency and maintain the ratio of the harvest which can help prevent exploitation of the *T. granosa*.

*Coastal Communities.* The result of this study would be beneficial for the coastal communities that are reliant on their source of income with aquaculture commodities like blood cockles. Maintaining the diversity and aspect ratio of male and female may increase the market value of blood cockle production since cockle aquaculture faces significant obstacles worldwide due to the fluctuating seed supplies and scarcity of broodstock from the wild (Miranda & Ferriols, 2023).

*Future Researchers.* The result of this study would serve as the basis for studies that involve sex identification in bivalves such as *T. granosa*. Some technologies are yet to be explored in machine learning and deep learning technologies that can lead to higher accuracy and distinguish the presence of sexual dimorphism in the *T. granosa*.



# Chapter 2

## Review of Related Literature

Aquaculture is the fastest-growing industry in animal food production and has great potential as a sustainable solution to global food security, nutrition, and development (*FAO 2024 Report: Sustainable Aquatic Food Systems Important for Global Food Security – European Fishmeal*, 2024). Aquaculture is deeply integrated into the livelihoods of Filipinos, not only through fish cultivation but also through the production of other aquatic species, including mollusks, oysters, clams, scallops, and mussels (Breton et al., 2017). Mollusks, particularly blood clams *Tegillarca granosa*, have economic and environmental significance. It has been a collective effort to maintain an ideal male-to-female ratio to avoid overharvesting and maintain the optimal ratio to preserve the population and production of the blood cockles.

The members of the Arcidae Family, including *T. granosa* are important sources of food and livelihood. Cockle aquaculture meets rising demands, however, it faces significant challenges due to fluctuating seed supplies (Miranda & Ferriols,

2023). To solve the problem, researchers exert a considerable amount of effort, developing a broader understanding of bivalves, including their sex-determining mechanism, due to their notable importance in terms of diversity, environmental benefits, and economic and market importance (Breton et al., 2017). Despite the promising idea of identifying sex, there is limited research reported in terms of sexual dimorphism, making it harder to distinguish through its morphological and morphometric characteristics.

By addressing the challenges in the sex identification of *T. granosa*, it would be able to address one problem at a time. Currently, there are no recent documented publications that integrate machine learning and deep learning in characterizing sexual dimorphism, reducing complexity, variability in sex determination, and differentiation mechanisms in bivalves, including *T. granosa* specifically.

## 2.1 Background on *T. granosa* and Their Importance

*Tegillarca granosa* (Linnaeus, 1758) is also known as blood cockles or blood clam. In the Philippines, it is known locally as Litob and Bakalan, a marine bivalve species from the family Arcidae. Litob is widely distributed in the world including Southeast Asia. They can be found in the intertidal mudflats adjacent to the mangrove forest (Srisunont, Nobpakhun, Yamalee, & Srisunont, 2020). With the intertidal mudflat as *T. granosa*'s habitat, they experience severe hypoxia or low oxygen levels in the blood tissues during the tidal cycle. The blood clams exhibit a unique red-blood phenotype where it serves two purposes the hemocyte

carries oxygen around the body and strengthens immune defenses. In addition, it possesses a unique ability to absorb oxygen at similar rates in water and air (Zhan & Bao, 2022).

*T. granosa* shell (refer to Figure 2.1) is medium-sized, fairly thick, ovate, and convex, with both valves being equal in size but asymmetrical from the hinge. The top edge of the dorsal margin is straight, while the front is rounded and slopes downward, with its back being obliquely rounded with a concave bottom edge. It has a narrow diamond-shaped ligament near the hinge with 3-4 dark chevron markings, although some may be incomplete. The shell's outer layer, or the periostracum, is smooth and brown with a straight hinge line and 40-68 fine short teeth arranged in a straight line. The beak, or prosogyrate, curves forward, with the shell having 18–21 raised ribs with blunt nodules and spaces between them. The inner shell is white with crenulations along the valves' ventral, anterior, and posterior margins. The posterior adductor scar is elongated and squarish, while the anterior adductor scar is similar but smaller in size. The mantle covering the bulk of *T. granosa*'s visceral mass is thin but the edges are thick and muscular. It bears the impression of the crenulated shell edges. Their foot is large with a ventral grove with no byssus or thread-like attachment. The *T. granosa*'s soft body is blood red (Narasimham, 1988).

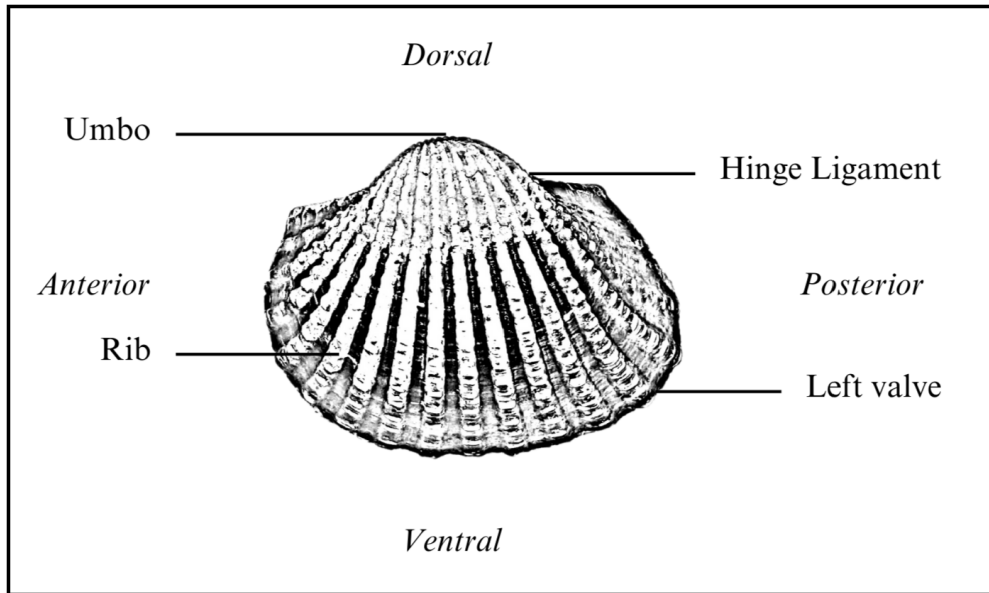


Figure 2.1: Diagram of *T. granosa*'s external anatomy.

*T. granosa* is one of the most well-known marine bivalves given that they are a protein-rich food, known for their rich flavor, substantial nutritional benefits, a good source of vitamins, low in fat, and contain a considerable amount of iron, important in combating anemia (Zha et al., 2022). Blood cockles were collected by locals inhabiting the brackish mudflats during the low tides for consumption and sold in the market as a source of livelihood (Miranda & Ferriols, 2023). *T. granosa* is not only valuable for its market and food purposes but also facilitates an important role in marine ecosystems as a food source for various organisms like wading birds, intertidal-feeding fish, and crustaceans such as shore crabs and shrimp (Burdon, Callaway, Elliott, Smith, & Wither, 2014). Blood cockles can act as sentinel species and a bioindicator of marine pollutants such as heavy metals (Ishak, Mohamad, Soo, & Hamid, 2016) and polycyclic aromatic hydrocarbons (PAHs) (Sany et al., 2014). Additionally, cockle shells can be utilized to create a cost-effective catalyst for biodiesel production by providing calcium oxide (Boey,

Maniam, Hamid, & Ali, 2011).

Determining the sex of bivalves is important for three reasons: diversity, environmental benefits, and economic significance (Breton et al., 2010). Firstly, with the estimated 25,000 living species under class Bivalvia, it would be a suitable resource to develop a broader understanding of their evolution of the sex and sex determination mechanism (Breton et al., 2010). Second, studying sex determination is important since bivalves are utilized as bioindicators of environmental health. This would pave the way for understanding bivalves' life cycle and population dynamics in determining different factors that affect them (Campos, Tedesco, Vasconcelos, & Cristobal, 2012). Thirdly, the immediate and practical reason to unveil the sex determination mechanism is the economic and nutritional importance of bivalves as a large population of people relies on fish and shellfish as sources of food and nutrition (Naylor et al., 2000). Additionally, male and female aquaculture commodities have different growth and economic values. Male Nile tilapia, for example, grow faster and have lower feed conversion rates than females, female Kuruma prawns (*Penaeus japonicus*) are generally larger than males at the time of harvest (Budd, Banh, Domingos, & Jerry, 2015).

Clearly, much more work is required to understand the mechanisms underlying sexual dimorphism in bivalves, specifically *T. granosa*. Just like the other aquaculture commodities, sex affects not just reproduction but it can also affect market preference and underlying economic value, making the determination of sex important for meeting consumer demands. These are the increasing significance of the *T. granosa* despite the lack of reviewed articles in the Philippines.

## 2.2 Sex Identification Methods in *T. granosa*

The current sex identification methods in *Tegillarca granosa* range from invasive histological techniques to less invasive methodologies like temperature-induced spawning. Each approach comes with its pros and cons regarding accuracy, feasibility, and impact on natural populations.

Induced spawning and larval rearing are considered the less invasive techniques used to study *T. granosa*. In the Philippines, limited research has been done on the *T. granosa* (Linnaeus, 1758), and this study, titled Initial Attempts on Spawning and Larval Rearing of the Blood Cockle, *T. granosa* in the Philippines, was conducted by Miranda and Ferriols (2023). The researchers conducted experiments on induced spawning and larval rearing, discovering that the eggs of female *T. granosa* were salmon pink, while the sperm released by males looked milky. After spawning, the researchers successfully generated 6,531,000 fertilized eggs.

The researchers highlighted the importance of *T. granosa* and other anadarinids as a food source established worldwide, especially in Malaysia and Korea. However, in the Philippines, the bivalve aquaculture of the clam species is still limited. The experiment, which focused on the culture and rearing of *T. granosa*, was attempted by subjecting the wild broodstocks to a series of temperature fluctuations to induce the spawning of gametes. This is currently the most natural and least invasive sex identification method for bivalves (Aji, 2011). The study of Miranda and Ferriols aimed to pave the way for the sustainable production of *T. granosa* seeds for aquaculture and stock enhancement, despite the scarcity of documented

hatchery culture of *T. granosa* from larvae to adults in the Philippines.

On the other hand, invasive techniques such as histological analysis offer a more thorough but harmful method for determining the sex of *T. granosa*. A study on the spawning period of blood cockle *T. granosa* (Linnaeus, 1758) in the Myeik coastal area examined 240 blood cockle samples for sex and gonad maturity stages using histological examination, with shell lengths ranging from 26–35 mm and shell weights from 8.1–33 g. For histological analysis, the whole soft tissues were removed from the shell and the flesh containing most parts of the gonads was fixed in formalin, dehydrated in an upgraded series of ethanol, and cleared in xylene. This invasive method allows for precise identification of the gonadal maturation stages based on cellular and structural changes in the gonads.

The classification of the gonad stages used was by Yurimoto et al. (2014). There are five maturation stages of gonadal development: immature (Stage I), developing (Stage II), mature (Stage III), spawning (Stage IV), and spent (Stage V) stages. The sex of the *T. granosa* was confirmed by the color of the gonad and by conducting a histological examination of the gonads. During the immature stage, sex determination was indistinguishable due to the difficulties of observing the germ cells. In the developing stage, the spermatocytes and a few spermatids can be seen for males, and immature oocytes are attached to the tube wall for the female. In the mature stage, the follicles are full of spermatozoa with their tails pointing towards the center of the tube for the male, and the female is full of mature oocytes that are irregular or polygonal in shape with the oval nucleus. Upon reaching spawning, some spermatozoa are released, causing the empty space in the follicle wall for males and females. There is a decrease in the number of mature oocytes and it exhibits nuclear disappearance due to the breakdown of

the germinal vesicle. Lastly, the spent stage is where the genital tube is deformed and devoid of spermatocytes which have completely spawned. In the female, the genital tube is deformed and degenerated, making it empty. The morphology of the cockle gonad shows that the area of the gonad increases according to the increased levels of gonad maturity. The coloration of the gonad tissue layer in the blood cockle varies from orange-red to pale orange in females and from white to grayish-white in males for different maturity stages (May et al., 2021).

Although the histological examination is the most reliable method for obtaining accurate information on the reproductive biology and sex determination of *T. granosa*, it has limitations. Given its invasive nature, this approach requires the dissection and destruction of specimens, making it unsuitable for continuous monitoring and conservation efforts. Moreover, the current understanding of sex determination in bivalves and mollusks is poor, and no chromosomes that can be differentiated based on their morphology have been discovered (Afiati, 2007). There exists a study that can provide insight into the sex-determining factor in bivalves but *N. schoberti* is more difficult to analyze concerning potential sexual dimorphism. Thickening the edges of the shell increases its inflation, which means the shell can hold more space inside. This extra space helps protandrous females accommodate more eggs.

## 2.3 Machine Learning and Deep Learning in Biology

Machine learning has the potential to improve the quality of life of human beings and has a wide range of applications in terms of research and development. The term machine learning refers to the invention and algorithm evaluation that enables pattern recognition, classification, and prediction based on models generated from available data (Tarcă, Carey, Chen, Romero, & Drăghici, 2007). The study of machine learning methods has advanced in the last several years, including biological studies. In biological studies, machine learning has been used for discovery and prediction. This section will explore existing machine learning studies that are applied in biological sciences, highlighting the identification of sex in shells, bivalves, and mollusks.

### 2.3.1 Deep Learning for Phenotype Classification in Ark Shells

In the study by Kim et al. (2024), the researchers utilized three (3) convolutional neural network (CNN) models: the Visual Geometry Group Network (VG-Gnet), the Inception Residual Network (ResNet), and the SqueezeNet. These deep learning models are utilized for the ark shells, namely *Anadara kagoshimensis*, *Tegillarca granosa*, and *Anadara broughtonii*, to identify the phenotype classification.

The researchers classified the ark shells based on radial rib count where they investigated the difference in the number of radial ribs between three species and

were counted. Their CNN-based model that classifies images of three ark shells can provide a theoretical basis for bivalve classification and enable the tracking of the entire production process of ark shells from catching to selling with the support of big data, which is useful for improving food safety, production efficiency, and economic benefits (Kim, Yang, Cha, Jung, & Kim, 2024).

### **2.3.2 Geometric Morphometrics and Machine Learning for Species Delimitation**

In *Geometric morphometrics and machine learning challenge currently accepted species limits of the land snail Placostylus (Pulmonata: Bothriembryontidae) on the Isle of Pines, New Caledonia*, the shell size was quantified using centroid size from the Procrustes analysis, and both the shape and size information were used in training the machine learning model. Their study concluded that the researchers support utilizing both methods: supervised and unsupervised machine learning, rather than choosing either of them individually. In general, their research contributes to the growing number of studies that have combined geometric morphometrics with the aid of machine learning, which is helpful in biological innovation and breakthrough (Quenu, Trewick, Brescia, & Morgan-Richards, 2020).

### **2.3.3 Contour Analysis in Mollusc Shells Using Machine Learning**

Tuset et al. (2020), in their study, *Recognising mollusc shell contours with enlarged spines: Wavelet vs Elliptic Fourier analyses*, mentioned that gastropod shells have

large spines and sharp shapes that differ based on environmental, taxonomic, and evolutionary influences. The researchers stated that classic morphometric methods may not accurately depict morphological features of the shell, especially when using the angular decomposition of the contour. The current research examined and compared the robustness of the contour analysis using wavelet transformed and Elliptic Fourier descriptors for gastropod shells with enlarged spines. For that, the researchers analyzed two geographically and ecologically separated populations of *Bolinus brandaris* from the NW Mediterranean Sea. Results showed that contour analysis of gastropod shells with enlarged spines can be analyzed using both methodologies, but the wavelet analysis provided better local discrimination. From an ecological perspective, shells with various sizes of spines in both areas indicate the broad adaptability of the species.

### 2.3.4 Machine Learning for Shape Analysis of Marine Organisms

In the study of Lishchenko and Jones (2021), titled *Application of Shape Analyses to Recording Structures of Marine Organisms for Stock Discrimination and Taxonomic Purposes*, they utilized geometric morphometrics (GM) as an approach to the traditional method of collecting linear measurements with the application of multivariate statistical methods and outline analysis in recording the structures of marine organisms. The main taxonomic categories (mollusks, teleost fish, and elasmobranchs) with their hard bodies have been used as an indication of age and a determinable time-scale and structure continue to go through life (Arkhipkin, 2005; Kerr & Campana, 2014). This study has explored variations in the mor-

photometry of recording structures in stock discrimination and systematics. The researchers utilized the principal component analysis rather than the traditional approach, which helps simplify the data without losing important information. They utilized landmark-based geometric morphometrics, which has three different types, namely: discrete juxtaposition of tissue, maxima or curvature, or other morphogenetic processes, and lastly, the extremal points are constructed landmarks.

Generalized Procrustes Analysis (GPA) is a common superimposition technique in landmark-based geometric morphometrics that aligns landmarks via translation, scaling, and rotation to eliminate non-shape deviations (Zelditch, Swiderski, & Sheets, 2004). However, there is a limit to the amount of smooth areas that may be captured, and it is possible to overlook significant shape details. Utilization of the semi-landmarks enhanced the shape description (Adams, Rohlf, & Slice, 2004). The researchers observed that using an outline-based approach would be more effective than using a landmark-based approach.

Another approach is the Fourier analysis which is a curve-fitting approach commonly used due to its well-known mathematical background and how general functions can be decomposed into trigonometric or exponential functions with definite frequencies. It has two main approaches, namely: Polar Transform (PT) in which it expresses the outline using equally spaced radii, and Elliptical Fourier Analysis (EFA) which separately analyzes the x and y coordinates of the shape. The PT works for simple rounded outlines and has the tendency to miss details in more complex shapes, unlike the EFA which can handle complex, convoluted outlines (Zahn & Roskies, 1972; Doering & Ludwig, 1990; Ponton, 2006). Many researchers view EFA as the most effective Fourier method for providing a comprehen-

hensive and detailed description of recording structures (Mérigot, Letourneau, & Lecomte-Finiger, 2007; Ferguson, Ward, & Gillanders, 2011; Leguá, Plaza, Pérez, & Arkhipkin, 2013; Mahé et al., 2016).

Landmark-based methods used in the study showed that there are detectable differences between male and female octopuses. However, the accuracy of determining sex based on these differences was low, similar to the results obtained with traditional morphometric techniques. The study involved a relatively small sample size of 160 individuals, and the structure being analyzed (the stylet, or internalized shell) varies significantly between individuals. Although the results aligned with findings from other studies that attempted to identify gender differences in cephalopods, the researchers concluded that the approach might not be accurate enough for reliable sex determination.

### 2.3.5 Deep Learning for Landmark-Free Morphological Feature Extraction

In another study, *a deep learning approach for morphological feature extraction based on variational auto-encoder: an application to mandible shape*, the Morpho-VAE machine learning approach was used to conduct a landmark-free shape analysis. Morpho-Vae reduces dimensions by concentrating on morphological features that distinguish data with different labels using an image-based deep learning framework that combines unsupervised and supervised machine learning. After utilizing the method in primate mandible images, the morphological features reveal the characteristics to which family they belonged. Based on the result, the method applied provides a versatile and promising tool for evaluating a wide range of image data of biological shapes including those missing segments.

### 2.3.6 Machine Learning for Sex Differentiation in Abalone

In the study, *Towards Abalone Differentiation Through Machine Learning*, researchers identified a problem in abalone farming which is having to identify the sex of abalone to apply measures for its growth or preservation. The researchers classified abalone sex using machine learning. Researchers trained the machine to classify different types of classes which are male, female, and immature. The results demonstrated the effectiveness of utilizing linear classifiers for this task.

Similarly, in the study, *Data scaling performance on various machine learning algorithms to identify abalone sex*, the researchers of the University of India (2022) focused on the data scaling performance of various machine learning algorithms to identify the abalone sex, specifically using min-max normalization and zero-mean standardization. The different machine learning algorithms are the Supervised Vector Machine (SVM), Random Forest, Naive Bayesian, and Decision Tree. Their study aims to utilize machine learning in terms of identifying the trends and distribution patterns in the abalone dataset. Eight features of the abalone dataset (length, diameter, height, whole weight, shucked weight, viscera weight, shell weight, ring) were used to determine the three sexes of Abalone. Their data has been grouped based on sex which are Female, Male, and Infant. They utilized the Synthetic Minority Oversampling Technique (SMOTE) in data balancing for the preprocessing of the data. Followed by data scaling or normalization where it converts numeric values in a data set to a general scale without distorting differences in the range of values. Then they classified by splitting the data into training and testing sets (Arifin, Ariawan, Rosalia, Lukman, & Tufailah, 2021).

The study found that Naive Bayes consistently performed better than other algo-

rithms. However, when applied to both min-max and zero-mean normalization, the average accuracies of the algorithms were as follows: Random Forest (62.37%), SVM with RBF kernel (59.49%), Decision Tree (57.20%), SVM with linear kernel (56.59%), and Naive Bayes (53.39%). Despite the performance decrease with normalization, Random Forest achieved the highest overall metrics, including an average balanced accuracy of 78.87%, sensitivity of 66.43%, and specificity of 83.31%. Liu et al. concluded that Random Forest is highly accurate because it can handle large, complex datasets, run processes in parallel using multiple trees, and select the most relevant features to enhance model performance (Arifin et al., 2021).

### 2.3.7 Machine Learning for Geographical Traceability in Bivalves

In the study, *BivalveNet: A hybrid deep neural network for common cockle (*Cerastoderma edule*) geographical traceability based on shell image analysis*, the researchers incorporated computer vision and machine learning technologies for an efficient determination of blood cockle harvesting origin based on the shell geometric and morphometric analysis. It aims to improve the traceability methodologies in these organisms and its potential as a reliable traceability tool. Thirty *Cerastoderma edule* samples were collected along the five locations on the Atlantic West and South Portuguese coast with individual images processed using lazy snapping segmentation, spectro-textural-morphological phenotype extraction, and feature selection through hybrid Principal Component Analysis and Neighborhood Component Analysis (Concepcion, Guillermo, Tanner, Fonseca, & Duarte, 2023).

The researchers developed a noninvasive image-based traceability technique, an

alternative to the chemical and biochemical analysis of the bivalves. It was able to incorporate machine learning methods to promote lesser human intervention. The researchers discovered that BivalveNet emerged as the superior model for bivalves with 96.91% accuracy which is comparable to the accuracy of the destructive methods with 97% and 97.2% accuracy rates. The result of the study aided the researchers in concluding that there is a possibility of on-site evaluation of the bivalve through the implementation of a mobile app that would allow the public and official entities to obtain information regarding the provenance of seafood products' traceability because of its noninvasive and image-based aspects (Concepcion et al., 2023).

*T. granosa* is known for having no sexual dimorphism. However, through several related studies, the researchers can apply how family shells of *T. granosa* have been identified based on its morphological and morphometric characteristics and the methods used in machine learning in identifying its sex.

## 2.4 Limitations on Sex Identification in *T. granosa*

To date, no distinction has been made between the male and female *T. granosa* in sexing methodology. In cockle aquaculture without clearly apparent sexual dimorphism, sexing can be performed using invasive methods such as chemical stimulation, dissection, and gonad-stripping. Induced spawning, specifically temperature shock, is the most natural and least invasive method for bivalves (Aji, 2011). However, the method (Wong & Lim, 2018) of immersing cockles in water

from hot to cold with a specific temperature requires deliberate and careful manipulation of the temperature over a specific period and would require constant management and monitoring.

Recent studies involved noninvasive methods, with a specific emphasis on morphological characteristics as indicators of sex differentiation. However, Tatsuya Yurimoto et al. (2014) stated that the existing methods for determining the sex of bivalves and mollusks in general are somewhat limited (Afiati, 2007). At present, there is no recorded evidence of sexual dimorphism in *T. granosa*. Gonochoristic is the classification given to *T. granosa* (Lee, 1997). However, Lee et al. (2012) reported that the sex ratio varied with shell length, suggesting that sex might alter.

Hermaphrodites can exhibit either sequential (asynchronous) or simultaneous (synchronous or functional) characteristics. Sequential hermaphrodites switch genders after being male or female for one or multiple yearly cycles. (Heller, 1993; Gosling, 2004; Collin, 2013). Sex change and consecutive hermaphroditism have been observed in different bivalve species, including Ostreidae, Pectinidae, Veneridae, and Patellidae. However, macroscopically differentiating bivalve sex is challenging. The only way it may be identified is through histological analysis of gonad remains but to do so there is an act of killing the organism (Coe, 1943; Gosling, 2004). Verification of sex change in bivalves to classify whether male or female while they are alive is challenging since they need to be re-confirmed and re-evaluated to be the same individual after a year.

Lee et al. (2012) found out that *T. granosa*, a species in Arcidae, has been discovered to be a sequential hermaphrodite, with the sex ratio changing with an

increase in the shell size. In bivalves, sex changes usually happen when the gonad is not differentiated between spawning seasons (Thompson, Newell, Kennedy, & Mann, 1996). But in *T. granosa*, after the spawning season, sex changes during its inactive phase. Results showed a 15.1% sex change ratio, with males having a higher sex change ratio (21.2%) than females (6.2%). The 1+ year class had a higher ratio (17.8%) than the 2+ year class (12.1%). Thus, this study indicates that *T. granosa* is a sequential hermaphrodite. The results of the study demonstrated that the bivalve's age affects the sex ratio and degree of sex change, but additional in-depth investigation is required to determine the role that genetic and environmental factors play in these changes.

No literature in the study of mollusks specifically addresses the machine learning and deep learning technologies used to determine the sex of *T. granosa* bivalves in various models. Nevertheless, various techniques such as shape analysis, morphometric analysis, Wavelet, and Fourier analysis, as well as different deep learning models like VGNet, ResNet, and SqueezeNet in CNN networks, are utilized for phenotype classification, while different machine learning algorithms could serve as the foundation for this research project.

## 2.5 Chapter Summary

This section summarizes the methodologies and problems discussed in other literature encompassing machine learning, deep learning, and other related bivalve studies.

Author	Technology / Method Used	Description of Problem	Pros	Cons
D. V. Miranda and V. M. E. N. Ferriols	Temperature shock	No recent studies are available on the production and rearing of <i>T. granosa</i> in the Philippines.	Employed less invasive techniques which minimize the stress in <i>T. granosa</i> and can lead to better survival rates.	Time-consuming as the entire process from fertilization to the spat stage took 120 days.
Karapunar, Baran and Werner, W. and Fürsich, F. T. and Nützel, A.	Morphometric analysis, microscope imaging, principal component analysis (PCA), and Fourier shape analysis	To address the observed shell dimorphism in the Early Jurassic bivalve <i>Nicanella rakoveci</i> , namely the presence or lack of crenulations on the ventral shell margin, and whether these variations represent sexual dimorphism and sequential hermaphroditism.	The methods used reveal significant morphological differences with regard to sexual dimorphism.	There could be misinterpretation of the shape differences of bivalves due to the constraints and resolution of technologies used.
K. May and C. Maung and E. Phyus and N. Tun	Histological examination	The need to understand the reproductive period of <i>T. granosa</i> in Myeik to ensure sustainable aquaculture and to prevent overexploitation.	Method used allows for accurate sex identification based on the histological characteristics and color of the gonads.	Invasive technique used to determine the sex of <i>T. granosa</i> through gonad histological analysis.
E. Kim and S.-M. Yang and J.-E. Cha and D.-H. Jung and H.-Y. Kim	Convolutional neural network (CNN) models, VGGNet, Inception-ResNet, SqueezeNet	Traditional methods of recognizing and classifying ark shell species based on shell traits are time-consuming and inaccurate.	Automated classification of the three ark shells using a deep learning model obtained an accuracy of 92.4%.	Challenges may arise with certain ark shells that share similar morphology.
Mathieu Quemu and S. A. Trewick and F. Brescia and M. Morgan-Richards	Neural network analysis (supervised learning) and Gaussian mixture models (unsupervised learning)	To determine whether the shape and size of the snail's shells can distinguish between two <i>Placostylus</i> species, particularly in groups that appear to be hybrids.	Combining geometric morphometrics and machine learning effectively answers biological issues, providing insights into species classification and possible hybridization.	Difficulty classifying intermediate phenotypes, with potential for overfitting and misclassification in both learning methods.
V. M. Tuset and E. Galimany and A. Farrés and E. Marco-Herrero and J. L. Otero-Ferrer and A. Lombarte and M. Ramón	Wavelet functions and Elliptic Fourier descriptors	Addresses the difficulty of accurately defining phenotypic diversity in gastropod shells.	Advanced contour analysis methods allow accurate differentiation of gastropod shell forms.	Cannot clarify the causes of phenotypic variation in the two populations studied.
Fedor Lishchenko and Jones, J. B.	Landmark- and outline-based Geometric Morphometric methods	To address difficulties in differentiating between stocks of marine organisms to prevent misidentification that could affect conservation and management.	Shape analysis improves taxonomic classification precision and offers close distinction between related species or organisms.	Landmark-based methods can be sensitive to landmark placement.
M. Tsutsumi and N. Saito and D. Koyabu and C. Furusawa	Morphological regulated variational AutoEncoder (Morpho-VAE)	The need for reliable, landmark-free methods, such as a modified variational autoencoder, to extract and decipher complex shapes from image data.	Employs dimension reduction and feature extraction, making it a user-friendly tool for biology non-experts.	Limited sample size in certain families presented challenges.
Barrera-Hernandez, R. and Barrera-Soto, V. and Martinez-Rodriguez, J. L. and Ríos-Alvarado, A. B. and Ortiz-Rodríguez, F.	Machine learning algorithms	Identifying the sex of abalones is challenging for producers applying specific growth or preservation strategies.	Machine learning algorithms accurately classify abalone sex into three categories: male, female, and immature.	Selected features may not fully capture the complexity of abalone morphology.
Concepcion, R. and Guillermo, M. and Tanner, S. E. and Fonseca, V. and Duarte, B.	EfficientNet-Bo, ResNet101, MobileNetV2, InceptionV3	Addresses the difficulty of accurately tracing bivalve harvesting origins using computer vision and machine learning algorithms to enhance seafood traceability and combat food fraud.	Non-invasive, image-based tools for bivalve traceability provide faster, cheaper, and equally accurate alternatives to traditional chemical analysis methods.	Small sample size (only 30 cockles) limits model reliability.

Table 2.1: Comparison of the methods used in bivalves studies.

Recent developments and breakthroughs in machine learning offer promising solutions to biological challenges. Research findings indicate that various deep learning techniques — such as convolutional neural networks (CNNs), geometric morphometrics, and other machine learning models — are effective in identifying phenotypes and determining the sex of various aquaculture species, including mollusks and abalones. These techniques provide a foundation for developing new, noninvasive methods to differentiate male and female *T. granosa*, potentially addressing the limitations of manual and invasive techniques. Thus, using machine learning to analyze morphological and morphometric features may streamline the process of sex identification.

Nevertheless, the use of machine learning and deep learning to determine the sex of *T. granosa* has not been fully explored. It lacks up-to-date and significant related literature on using machine learning and deep learning to identify sex in *T. granosa*, particularly given the species' possible sequential hermaphroditism and lack of obvious external sexual distinctions.

# Chapter 3

## Research Methodology

This chapter discusses the materials and methods employed, focusing on the detailed workflow in conducting the study from sample collection, preprocessing, model training and evaluation.

Dr. Victor Emmanuel Ferriols, the director of the Institute of Aquaculture, oversaw the overall workflow by providing baseline characteristics of the samples that the researchers could focus on. Additionally, guidance was offered by the research associates Allena Esther Artera and LC Mae Gasit. Consequently, the entire dataset collection process was conducted at the University of the Philippines Visayas hatchery facility.

The methodology consisted of nine parts: (1) Sample Collection, (2) Ethical Considerations, (3) Creating *T.granosa* Dataset, (4) Morphological Characteristics Collection (5) Image Acquisition and Pre-processing, (6) Hardware and Software Configuration, (7) Machine Learning for Morphometric Data, (8) Deep Learning

for Morphological Analysis, and (9) Evaluation Metrics

### 3.1 Sample Collection

The collection of *T. granosa* samples used in this study was part of an ongoing research project by UPV DOST-PCAARRD titled "Establishment of the Center for Mollusc Research and Development: Development of Spawning and Hatchery Techniques for the Blood Cockle (*Anadara granosa*) for Sustainable Aquaculture." A total of 271 samples were provided for this study to classify the sex of *T. granosa*. The samples, ranging in size from 34 to 61 mm, were sourced from the coastal area of Zarraga, Iloilo, and fish markets in Ivisan, Capiz, Philippines (see Figures 3.1 and 3.2).

The research and experimentation were conducted at the University of the Philippines Visayas hatchery facility in Miagao, Iloilo, where the samples were maintained in 200 L fiberglass-reinforced plastic (FRP) tanks containing filtered seawater with 35 ppt salinity (Miranda & Ferriols, 2023).

As part of the data collection process, the researchers utilized induced spawning and dissection to classify the sex of the samples. Induced spawning through temperature fluctuations was the most natural and least invasive method for bivalves compared to other approaches (Aji, 2011). However, since not all samples exhibited gamete release, the researchers also performed dissections, assisted by hatchery staff, to expedite data collection. The sex of the dissected samples was identified based on the coloration of gonad tissue, which varies according to sex and maturity stage. Females exhibited orange-red to pale orange gonads, while

males displayed white to grayish-white gonads (May et al., 2021).

The methods used for data collection were considered noninvasive, given that *T. granosa* are oxygen regulators well adapted to tidal exposure and hypoxia (Davenport & Wong, 1986).



Figure 3.1: Female *T. granosa* shells.



Figure 3.2: Male *T. granosa* shells.

## 3.2 Ethical Considerations

The ongoing research project titled "Establishment of the Center for Mollusc Research and Development: Development of Spawning and Hatchery Techniques for the Blood Cockle (*Anadara granosa*) for Sustainable Aquaculture"—from which the samples used in this study were obtained—was reviewed and approved by the Institutional Animal Care and Use Committee (IACUC) of the University of the Philippines Visayas.

### 3.3 Creating *T. granosa* Dataset

The experiment began with the collection of preliminary observations from 100 *T. granosa* samples. For the actual experimentation, the researchers collected the full dataset in batches until a total sample size of 271 *T. granosa* was reached. Linear measurements—including width, height, length, rib count, hinge line length, and the distance between the umbos—were recorded and organized into a CSV file. This dataset served as the foundation for training and testing machine learning models, as well as for establishing a baseline for the convolutional neural networks.

Images of each sample were captured and saved in JPEG format using a standardized file naming convention that included the sample’s sex, the shell’s orientation or view, and its corresponding number out of the 271 total samples. File names for female *T. granosa* samples began with “0”, while those for male samples began with “1”. Each file name also included one of the six captured views: (1) dorsal, (2) ventral, (3) anterior, (4) posterior, (5) left lateral, and (6) right lateral (*refer to Figure 3.3*), followed by a unique sample number. For example, “010001” denoted the first female sample taken from the dorsal view, while “110001” represented the first male sample from the same view. This naming convention was implemented to prevent data leakage and ensure accurate labeling of images according to their respective samples.

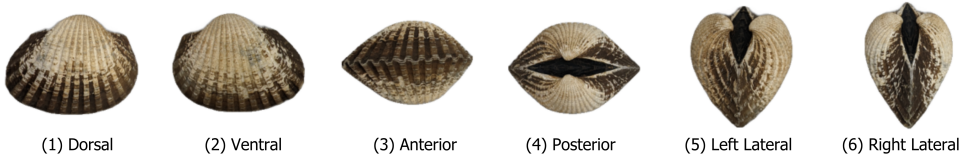


Figure 3.3: Different views of the *T. granosa* shell captured.

## 3.4 Morphometric Data Collection

Morphology refers to biological form and is one of the most visually recognizable phenotypes across all organisms (Tsutsumi, Saito, Koyabu, & Furusawa, 2023). In this study, morphological characteristics describe the structural features of *T. granosa*, focusing on measurable attributes such as shape and size. Morphometric characteristics, on the other hand, refer to specific quantifiable features of *T. granosa*, including length, width, height, hinge line length, distance between the umbos, and rib count. Quantifying and characterizing these traits is essential for understanding and visualizing variations in *T. granosa*'s morphology.

The researchers measured the height, width, and length of *T. granosa* using a Vernier caliper with a precision of up to 0.01 mm. Refer to Figure 3.4 for the corresponding measurement diagram. Length (A) refers to the distance from the anterior to the posterior of the shell. Width (B) is defined as the widest span across the shell from the left to the right valve. Height (C) measures the distance from the base to the apex of the shell. In addition, the hinge line length (D) near the hinge and the distance between the umbos (E) were recorded.

Reyment and Kennedy (1998) emphasized that including rib count (F) as supplementary information can enhance identification accuracy. Following this insight, the researchers also recorded the rib count for both male and female *T. granosa*, adjusting the values by calculating ratios to account for natural size variation among specimens.

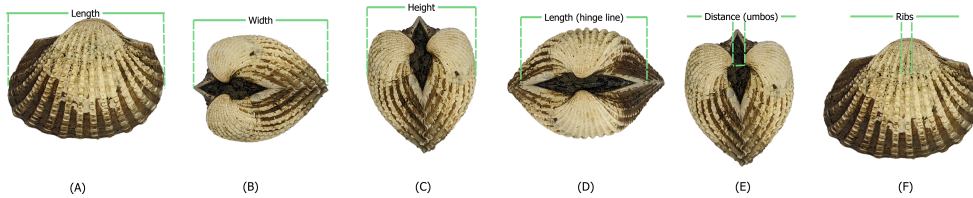


Figure 3.4: Linear measurements that were gathered from the shell of *T. granosa*.

### 3.5 Image Acquisition and Data Gathering

This study comprised 144 male and 127 female *T. granosa* samples, resulting in a total of 1,626 images captured from various angles. To ensure consistency during image acquisition, a box-like structure with a white background was constructed to control the imaging environment (*see Figure 3.5*).

The images were captured using a Google Pixel 3 XL smartphone, which features a resolution of  $2960 \times 1440$  pixels and a 12.2 MP camera ( $4032 \times 3024$  pixels). Additional camera specifications include an f/1.8 aperture, 28mm wide lens,  $\frac{1}{2.55}$ " sensor size, 1.4 $\mu$ m pixel size, dual-pixel phase detection autofocus (PDAF), and optical image stabilization (OIS) (Concepcion et al., 2023).



Figure 3.5: Image acquisition setup for *T. granosa* samples.

## 3.6 Hardware and Software Configuration

This section discusses the software, programming languages, and tools used for sex identification. Data collection, preprocessing, and model training were conducted on a Windows 11 operating system using an ACER Aspire 3 general-purpose unit (GPU) equipped with an AMD Ryzen 3 7320U CPU with Radeon Graphics (8 cores) @ 2.395 GHz and 8 GB of RAM. Google Colaboratory was utilized for collaborative preprocessing, computer vision tasks, and model training. Image preprocessing was performed using computer vision techniques in Python, while machine learning and deep learning models were developed using Python libraries, including Keras. The results of the gathered measurements were stored and managed using spreadsheet software. GitHub was employed for version control, documentation, and activity tracking throughout the study.

## 3.7 Machine Learning on Morphometric Data

This section discusses the machine learning operations that served as a baseline prior to implementing more complex deep learning methods for image classification. The study utilized collected variables including linear measurements—length, width, height, hinge line length, distance between the umbos, and rib count—along with derived features used as predictors. These included the length-to-width ratio, length-to-height ratio, width-to-height ratio, umbos distance-to-length ratio, hinge line length-to-length ratio, umbos distance-to-height ratio, and rib density. The samples were classified by sex, with females labeled as 0 and males as 1, which served as the response variable.

### 3.7.1 Data Preprocessing

The preprocessing of the dataset involved several essential steps, carried out using Python in Google Colaboratory, in preparation for machine learning analysis (see *Figure 3.6*).

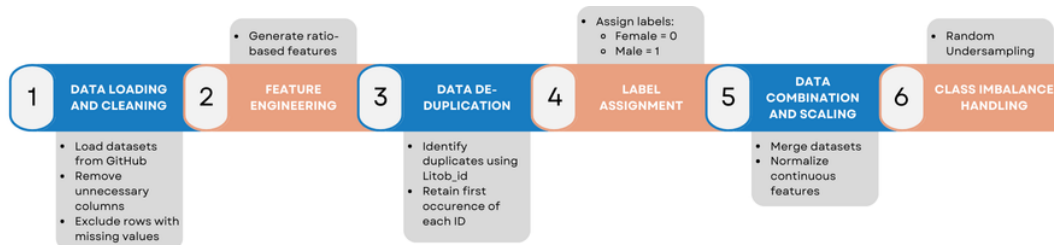


Figure 3.6: Data preprocessing in machine learning pipeline.

#### ***Data Loading and Cleaning***

The process began by loading two separate datasets for male and female *T. granosa*

directly from GitHub using `pd.read_csv()`. Unnecessary columns were removed, and rows containing missing values were excluded using the `dropna()` function to ensure data completeness and reliability.

### ***Feature Engineering***

Additional ratio-based features were generated to augment the existing measurements. These included the length-to-width ratio, length-to-height ratio, width-to-height ratio, hinge line length-to-length ratio, umbos distance-to-length ratio, umbos distance-to-height ratio, and rib density. These derived features aimed to emphasize shape characteristics independent of size, improving the models' ability to distinguish morphological differences between sexes.

### ***Data De-duplication***

To avoid redundancy and ensure each specimen was uniquely represented, the last three digits of each `Litob_id` were used to identify duplicates. Only the first occurrence of each unique ID was retained, reducing potential bias caused by repeated entries.

### ***Label Assignment***

A new column labeled `Label` was added to both datasets. Female specimens were assigned a label of 0, and male specimens a label of 1. This column served as the target variable for classification.

### ***Data Combination and Scaling***

After cleaning and feature engineering, the male and female datasets were merged into a single DataFrame. The `Litob_id` column was removed post de-duplication.

All continuous numeric features were normalized using `MinMaxScaler` to scale values to the range [0, 1].

Rib count was excluded from normalization because it is a discrete feature with biologically meaningful bounds. According to best practices in machine learning, normalizing discrete or categorical features can distort their meaning and is often unnecessary (Jaiswal, 2024). In this study, rib count was treated as a categorical attribute due to its biological significance and finite, non-continuous nature.

### ***Class Imbalance Handling***

After normalization, class imbalance was addressed by applying Random Undersampling to the male dataset. This technique randomly reduced the number of male samples to match the number of female samples (127 each), ensuring equal class representation. By using this approach, model bias was minimized, and the classification performance became more reliable across both classes.

### **3.7.2 Machine Learning Models Training**

#### ***Model Selection and Hyperparameter Tuning***

To establish a baseline for classification, various models were evaluated: Logistic Regression, K-Nearest Neighbors, Support Vector Machine, Random Forest, AdaBoost, Extra Trees, and Gradient Boosting. Hyperparameter tuning was conducted using `GridSearchCV`, which systematically identified the optimal settings for each model to enhance accuracy and performance.

### Cross-Validation

A five-fold cross-validation approach was implemented (*refer to Figure 3.7*). The dataset was divided into five subsets, with four used for training and one for validation. This process was repeated five times, with each fold serving as the validation set once. This method ensured that model evaluation was robust and generalizable, minimizing the bias that may result from a single train-test split.  
 (GeeksforGeeks, 2024)

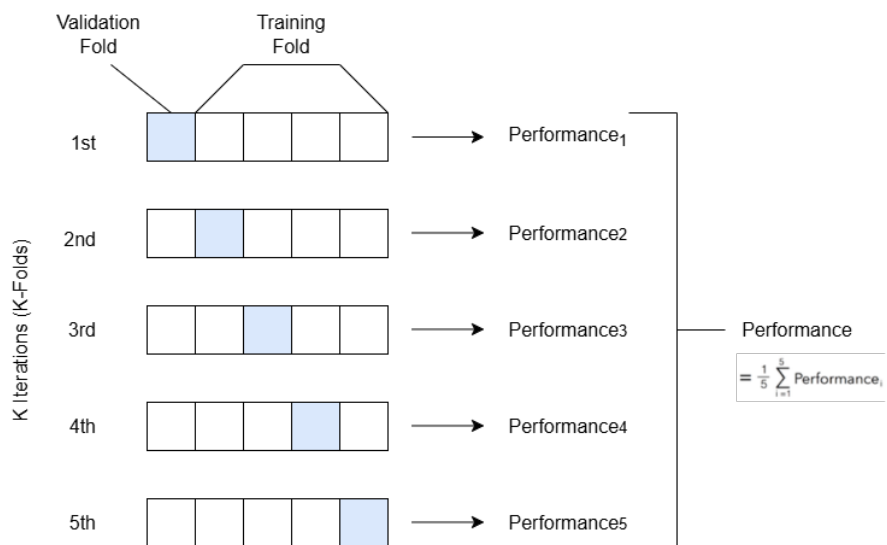


Figure 3.7: Diagram of k-fold cross-validation with  $k = 5$ .

## 3.8 Deep Learning for Morphological Analysis

This section outlines the application of deep learning techniques in analyzing the morphological characteristics of *Tegillarca granosa* to identify their sex based on shell images. A convolutional neural network (CNN) architecture was implemented and trained on preprocessed images using stratified cross-validation.

### 3.8.1 Image Preprocessing

This subsection details the image processing techniques applied to raw shell images of *T. granosa* using computer vision methods before training the deep learning model. The image preprocessing techniques include standardizing input dimensions and removing shadows, background, and noise. Image preprocessing ensures consistent and high-quality input data for model training.

#### *Adjusting Dimensions*

All images were resized to a consistent dimension of 256x256 pixels to ensure uniformity throughout the dataset. This standardization is essential for CNNs, as a consistent input dimension is required. While resizing, the aspect ratio was maintained to prevent distortion of the morphological features, and padding was added to retain the original format.

#### *Background Removal*

Background removal was performed to maintain a consistent white background throughout the dataset. The tool `rembg` was used to efficiently remove the original

background, retaining the foreground from the raw images. This method resulted in clear images with a white background, enhancing focus on the morphological features and defining the shell boundaries.

### ***Shadow Removal***

To minimize noise caused by shadows around the shell, HSV thresholding, contours, and morphological thresholds were applied to isolate and remove shadowed regions. This approach preserved the natural color of the blood cockles and eliminated shadows and noise from the surrounding area (*see Figures 3.8 and 3.9*).



Figure 3.8: Shadows removed from male samples at different angles.



Figure 3.9: Shadows removed from female samples at different angles.

### 3.8.2 Convolutional Neural Network

Convolutional Neural Networks are the deep learning tool used in image classification, specifically binary classification. CNNs leverage their ability to share weights and use pooling techniques, reducing the number of parameters (Cui, Pan, Chen, & Zou, 2020). The proposed CNN architecture for sex identification of blood cockles employs 5 layers, designed to extract features from the input image with dimensions. The layers consist of three convolution layers, a pooling layer, a flatten layer, dropout, and two dense layers. The CNN framework used in this study was adapted from an open source GitHub implementation by Christian Versloot, which focused on K-fold Cross Validation using TensorFlow and Keras, which was customized to align with the objectives of this study. The overall framework is illustrated in Figure 3.10.

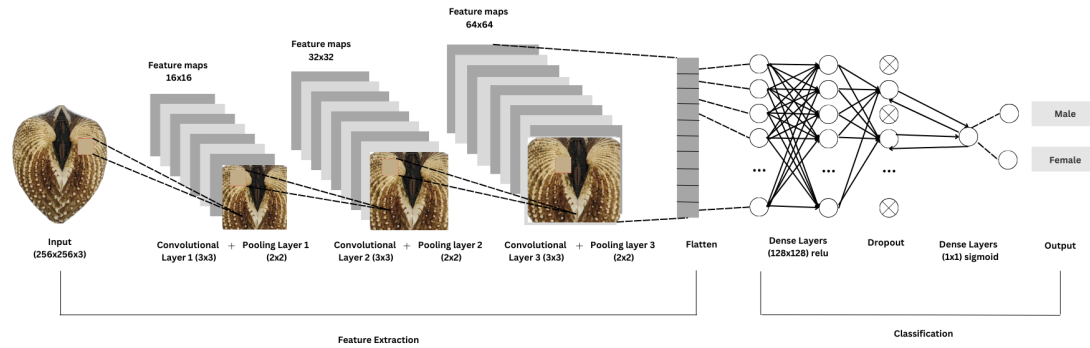


Figure 3.10: Architecture of convolutional neural network (CNN).

#### ***Convolution Layer***

The convolution layers of CNN extract the features from the input image through the convolution operation. This study uses three convolution layers with a 3x3 kernel size and filter sizes of 16, 32, and 64 (*refer to Table 3.1*). The first layer extracts the low-level features, such as edges, lines, and corners, while the deeper

layers iteratively extract more complex information from these low-level features. The ReLU activation function is used as the baseline for this model, and experiments are conducted with different activation functions, such as ELU and PReLU, to evaluate their impact on learning complex patterns within the data.

### ***Pooling Layer***

A pooling layer was added after the convolution layer to enhance calculation speed and prevent overfitting (Cui et al., 2020). In this study, max pooling was applied with a (2,2) kernel size.

### ***Fully Connected and Dropout***

Fully connected layers follow after the convolution and pooling layers. Each neuron connects to all neurons of the previous layer. The output values from the fully connected layers are sent to an output layer. It was classified using different sigmoid functions appropriate for binary classification.

A large number of parameters in the training process can lead to overfitting. It occurs when the model learns the training data too well, including its noise and irrelevant details. This results in poor performance on unseen data. To mitigate the overfitting, the dropout layer was employed. Dropout works by temporarily discarding a portion of the neurons in the network with probability  $p$  ( $0 < p < 1$ ). During this process, these neurons do not participate in the forward propagation process of CNN and the backward propagation process (Cui et al., 2020).

Layer	Number of Neurons	Stride	Kernel Size	Activation	Parameters
Rescaling					
Convolution	16	1x1	3x3	ReLU	448
Max Pooling		1x1	2x2		
Convolution	32	1x1	3x3	ReLU	4,640
Max Pooling		1x1	2x2		
Convolution	64	1x1	3x3	ReLU	18,496
Max Pooling		1x1	2x2		
Flatten					
Dense	128			ReLU	7,372,928
Dropout					
Dense	1			Sigmoid	129

Table 3.1: Architecture of the convolutional neural network used.

### 3.8.3 CNN Training

The dataset consists of 1626 images, with 127 samples from females and 144 samples from males, individually for each angle. Given the minimal class imbalance, random undersampling was carried out to create a balanced dataset. All images were resized to 256x256 pixels and normalized using a Rescaling layer, ensuring pixel values were within the range [0, 1].

#### *Data Splitting*

Due to the limited dataset size, a traditional train-test split was not adopted. Instead, a 5-fold stratified cross-validation approach was used to maximize the use of available data while preserving the class distribution within each fold (*refer to Figure 3.11*). `StratifiedKFold` was applied to ensure that the distribution of male and female samples remained consistent across all folds, thereby enabling fair and robust model evaluation (GeeksforGeeks, 2020).

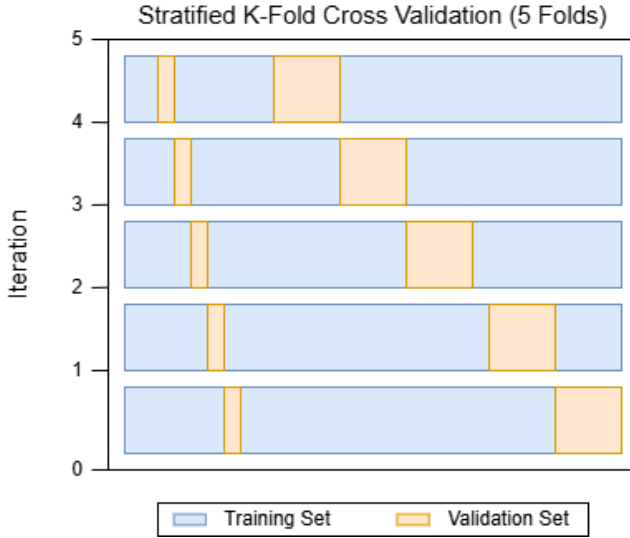


Figure 3.11: Diagram of stratified k-fold cross-validation with  $k=5$ .

### **Data Augmentation**

Before model training, on-the-fly data augmentation (OnDAT) was applied exclusively to the training data within each fold, generating augmented data during each iteration. The augmentations included random horizontal flips, slight rotations (0.05), and zoom transformations (0.05)(Awan, 2022). This approach exposed the model to constantly changing data variations, allowing better exploration of the underlying data generation process and reducing the risk of overfitting spurious patterns (Cerqueira, Santos, Baghoussi, & Soares, 2024).

When data augmentations were applied randomly and on-the-fly, the model encountered slightly different versions of the same 254 male and 254 female images in each epoch. This enhanced the diversity of the dataset and improve model generalization. All augmentation was strictly limited to the training subset of each fold to prevent data leakage and maintain the validity of the results (*Figure 3.12*).

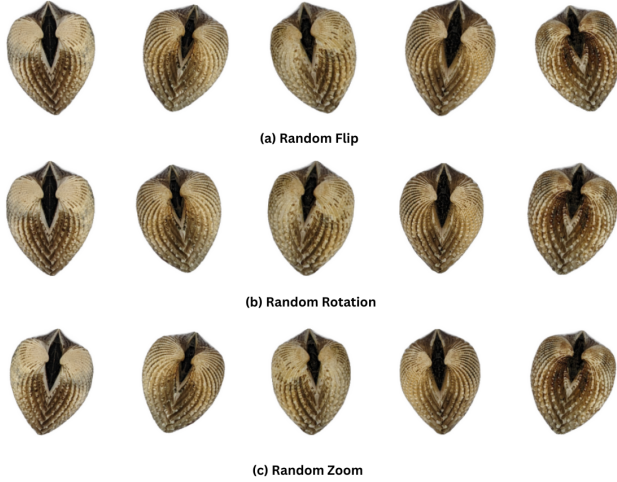


Figure 3.12: On-the-Fly dataset augmentation (OnDAT) techniques.

### ***Training Procedure***

During the training process, model performance per fold was carefully monitored. One important thing to observe is the consistency in the performance, whether the model is still learning or is at high risk of overfitting. Early stopping was applied to ensure the stable performance of the model across folds. This technique allows for monitoring the training of the neural network, stopping when the performance metrics, in this case, validation loss, cease to improve. Furthermore, to enhance the learning process, `ReduceLROnPlateau` was applied, which decreased the learning rate if there was no improvement in the model for a specified number of epochs and restores model weights from the end of the best epoch in every fold (Team, n.d.).

The model was trained using the Adam optimization algorithm, with an initial learning rate of 0.001. Binary cross-entropy, commonly known as the log loss, was employed as the loss function due to its effectiveness in binary classification tasks. To reduce the risk of overfitting, a dropout rate of 0.5 was applied, ran-

domly deactivating half of the neurons during the training process to improve generalization.

### 3.9 Evaluation Metrics

Evaluating the performance of a binary classification model is essential, and selecting appropriate metrics depends on the specific requirements of the user. The performance of both supervised machine learning and deep learning models will be measured using several key metrics, including accuracy, precision, recall, F1 Score, and the area under the receiver operating characteristic curve (AUC-ROC) score.

Accuracy (ACC) is the ratio of the overall correctly predicted samples to the total number of examples in the evaluation dataset (Cui et al., 2020). It measures the overall correctness of the model in predicting both male and female blood cockles. This metric provides insight into how well the model performs across all classifications. The formula for accuracy is:

$$\text{ACC} = \frac{\text{Correctly classified samples}}{\text{All samples}} = \frac{TP + TN}{TP + FP + TN + FN} \quad (3.1)$$

where:

TP or true positive is the number of male samples that were correctly identified as male *T. granosa*,

TN or true negative is the number of female samples that were correctly identified as female *T. granosa*,

FP or false positive is the number of female samples that were incorrectly identified as male *T. granosa*, and

FN or false negative is the number of male samples that were incorrectly identified as female *T. granosa*.

Precision (PREC) is the ratio of correctly predicted positive samples to all samples assigned to the positive class (Cui et al., 2020). This metric helps in evaluating the fairness of the model and prevents the misclassification of blood cockles as it identifies potential inaccuracies or biases. The formula for precision is:

$$\text{PREC} = \frac{\text{True positive samples}}{\text{Samples assigned to positive class}} = \frac{TP}{TP + FP} \quad (3.2)$$

Recall (REC), also known as sensitivity or the true positive rate (TPR), is the ratio of correctly predicted positive cases to all the actual positive samples (Cui et al., 2020). It represents the ability of the model to correctly identify positive male and female samples. The formula for recall is:

$$\text{REC} = \frac{\text{True positive samples}}{\text{Samples classified positive}} = \frac{TP}{TP + FN} \quad (3.3)$$

The F1 Score is the harmonic mean of precision and recall, which penalizes extreme values of either of the two metrics (Cui et al., 2020). It is particularly useful when the class distribution is imbalanced. The formula for the F1 Score is:

$$\text{F1} = \frac{2 \times \text{precision} \times \text{recall}}{\text{precision} + \text{recall}} = \frac{2 \times TP}{2 \times TP + FP + FN} \quad (3.4)$$

The AUC-ROC is a performance measurement for classification problems. The receiver operating characteristic (ROC) curve is a plot of the true positive rate (recall) against the false positive rate (1 - specificity), and the area under the curve (AUC) score quantifies the overall ability of the model to discriminate between positive and negative classes. A higher AUC indicates better model performance. (Nahm, 2022)



# Chapter 4

## Results and Discussions

This chapter presents the results from the machine learning and deep learning analyses conducted on the preprocessed dataset. It includes an evaluation of various machine learning classifiers and the application of deep learning models for image-based classification. The primary focus is on identifying key predictors and assessing classification performance for sex identification in *T. granosa*.

### 4.1 Machine Learning Analysis

This chapter outlines the results of preprocessing, training of machine learning models, and feature importance analysis, all conducted in Google Colab using Python. The dataset was preprocessed in Colab, and the training and evaluation of various classifiers were performed entirely within this environment. This part of the paper includes five subsections: data exploration, statistical analysis, feature importance analysis, performance evaluation, and visualizations for machine

learning.

### 4.1.1 Data Exploration

Exploratory data analysis was performed to characterize the dataset using data to understand underlying patterns and behaviors using descriptive statistics and correlation heatmap. A correlation heatmap was created to assess the relationship between the predictors and the target variable.

The heatmap (see *Figure 4.1*) revealed three features most correlated with the sex of *T. granosa*: the width-height ratio ( $r = 0.18$ ), the umbos distance-length ratio ( $r = 0.12$ ), and the distance between the umbos ( $r = 0.12$ ). Each of these features demonstrated a weak positive relationship with the target variable.

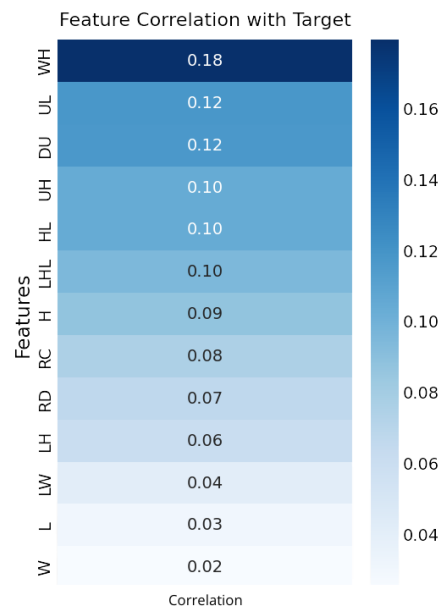


Figure 4.1: Heatmap of morphometric correlations with *T. granosa* sex.

### 4.1.2 Statistical Analysis

#### *Descriptive Statistics*

Descriptive statistics summarize and describe the main characteristics of a dataset, offering a concise overview of its features. Table 4.1 provides a comparison of the morphometric features of *T. granosa* between male and female samples. Generally, male *T. granosa* have slightly longer shells (mean = 51.69 mm) than females (mean = 50.24 mm). However, female *T. granosa* exhibits marginally greater shell height and width. These observations suggest that male shells are more elongated, while female shells appear more rounded or inflated.

The rib count and rib density are nearly identical between the sexes, indicating that these features might not be significant indicators for distinguishing between males and females. However, noticeable differences are observed in hinge line length and the distance between umbos. Female *T. granosa* exhibits longer hinge lines (mean = 31.97 mm) and a greater umbo distance (mean = 4.05 mm) than males, which could point to structural differences in shell formation related to sex.

In terms of the shape of *T. granosa*, the calculated ratios offer additional insight. Males have slightly higher length-to-width and length-to-height ratios, reinforcing that their shells are more elongated. In contrast, females exhibit slightly higher umbo-related ratios, such as umbo distance-to-height and umbo distance-to-length, suggesting a more prominent umbo or hinge area.

Looking at the standard deviations, male specimens demonstrate greater variability in certain features—particularly in shell length, where the standard deviation is notably higher (31.75) than that of females (7.49). This suggests that male *T.*

*granosa* exhibits a wider range of sizes. While the differences are subtle, features like shell length, hinge line length, and specific shape ratios may be useful inputs for developing a machine learning model for sex classification.

Feature	Male Mean	Female Mean	Male SD	Female SD
Length	51.69	50.24	31.75	7.49
Width	37.69	37.95	5.13	5.66
Height	33.85	34.74	4.98	5.18
Rib Count	19.87	19.74	0.85	0.84
Hinge Line Length	30.81	31.97	5.96	6.27
Umbos Distance	3.50	4.05	1.50	3.08
LW Ratio	1.39	1.33	1.06	0.08
LH Ratio	1.54	1.45	0.98	0.08
WH Ratio	1.11	1.09	0.07	0.06
UL Ratio	0.07	0.08	0.02	0.06
HL Ratio	0.62	0.63	0.07	0.06
UH Ratio	0.10	0.12	0.04	0.09
Rib Density	0.40	0.40	0.06	0.06

Table 4.1: Comparison of morphometric features between male and female *T. granosa*, showing mean and standard deviation (SD) values.

### **Mann-Whitney U Test**

As part of the exploratory data analysis, statistical testing confirmed that the dataset did not follow a normal distribution (see Table 4.2). Consequently, the Mann-Whitney U test was applied with a significance level of  $\alpha = 0.05$  to compare male and female samples. Out of thirteen features, five showed statistically significant differences. These included: width-height ratio ( $p = 0.003$ ), length-width ratio ( $p = 0.011$ ), umbos distance-length ratio ( $p = 0.019$ ), distance between umbos ( $p = 0.025$ ), and umbos distance-height ratio ( $p = 0.036$ ).

It is important to note that statistical significance does not imply predictive importance. Therefore, further analysis, such as feature importance evaluation, was

performed to identify the most informative predictors for classification.

Variable	p-value
WH_ratio	0.003
LW_ratio	0.011
UL_ratio	0.019
Distance Umbos	0.025
UH_ratio	0.036
HL_ratio	0.079
Length (Hinge Line)	0.120
Height	0.124
Rib Density	0.181
Rib count	0.251
Length	0.334
LH_ratio	0.490
Width	0.753

Table 4.2: Mann-Whitney U test results for sex-based feature comparison.

### 4.1.3 Feature Importance Analysis

Feature importance was assessed using the Kruskal-Wallis test, a non-parametric method that is suitable for evaluating differences in distributions across groups when the data does not follow a normal distribution. This approach was chosen because of the non-normality of the dataset and its robustness in handling continuous and ordinal data without assuming homogeneity of variances. (Ribeiro, 2024)

Kruskal-Wallis test analysis showed that the width-to-height ratio (WH ratio) had the highest importance score, indicating it is the most statistically significant feature for distinguishing the sex of *T. granosa*. Other notable features included the length-to-width ratio (LW ratio), umbos distance-to-length ratio (UL ratio), distance between the umbos, and umbos distance-to-height ratio (UH ratio), all

of which contributed significantly to the classification task (*refer to Figure 4.2*).

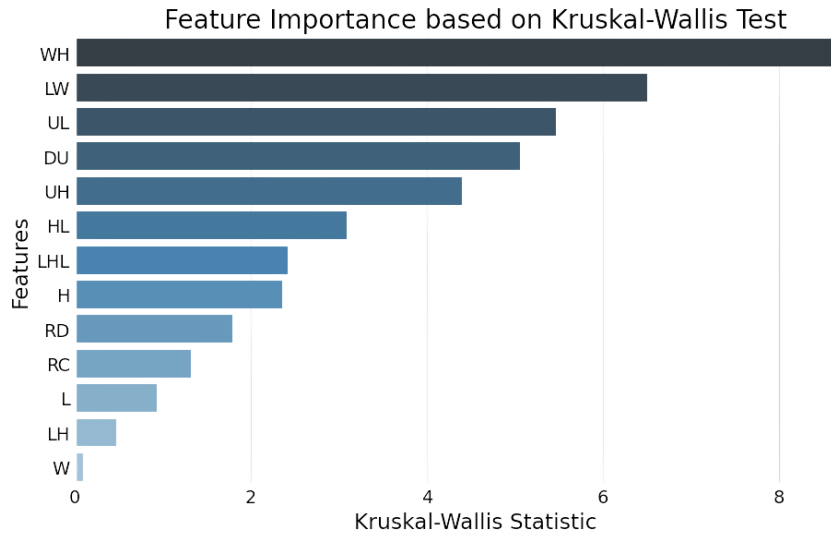


Figure 4.2: Feature importance scores using the Kruskal-Wallis test.

#### 4.1.4 Performance Evaluation

Table 4.3 shows the performance metrics of different machine learning models trained using all 13 features from the dataset. Among the models, Gradient Boosting achieved the highest accuracy of 61.03%, along with strong precision, recall, and F1 Score values. AdaBoost also performed competitively, with an accuracy of 60.63%. These results highlight the effectiveness of ensemble methods such as Gradient Boosting and AdaBoost when utilizing the full feature set, likely because of their capability to combine multiple weak learners into a more robust predictive model (Hussain & Zaidi, 2024).

Model	Accuracy (%)	Precision (%)	Recall (%)	F1 Score (%)
Support Vector Machine	58.62	58.62	58.62	58.44
Logistic Regression	57.83	57.83	57.83	57.61
K-Nearest Neighbors	51.18	51.31	51.18	50.77
Extra Trees	59.07	59.54	59.07	58.45
Random Forest	59.85	59.99	59.85	59.80
Gradient Boosting	61.03	61.32	61.03	60.81
AdaBoost	60.63	60.98	60.63	60.39

Table 4.3: Performance metrics for models with all 13 features.

Table 4.4 presents the performance of the same models using only the top five features identified through Kruskal-Wallis feature importance analysis. The selected features are the distance between the umbos, length-to-width ratio, width-to-height ratio, umbos distance-to-height ratio, and umbos distance-to-length ratio.

Interestingly, the overall performance of the models improved when using only the top 5 features compared to using all 13. KNN achieved the best results with an accuracy of 64.16%, precision of 64.97%, recall of 64.16%, and an F1 Score of 63.75%. Gradient Boosting followed closely behind. These findings suggest that reducing the feature set to the most relevant variables helped simplify the models, improved generalization, and enhanced predictive performance—particularly for KNN, which showed a notable improvement over its earlier results with the full feature set.

Model	Accuracy (%)	Precision (%)	Recall (%)	F1 Score (%)
Support Vector Machine	63.77	64.47	63.77	63.42
Logistic Regression	63.75	63.87	63.75	63.70
K-Nearest Neighbors	64.16	64.97	64.16	63.75
Extra Trees	61.04	61.68	61.04	60.67
Random Forest	61.01	61.12	61.01	60.91
Gradient Boosting	64.15	64.24	64.15	64.01
AdaBoost	61.02	61.26	61.02	60.82

Table 4.4: Performance metrics for models with 5 features.

### 4.1.5 Visualizations for Machine Learning

Figure 4.3 is a confusion matrix that summarizes the performance of the KNN model in classifying *T. granosa* based on their sex, where 0 represents female samples and 1 represents male samples. From the matrix, it can be observed that out of all the actual female samples (true label 0), 91 were correctly predicted as female (true positive for class 0), while 36 were incorrectly classified as male (false negative for class 0). On the other hand, out of all the actual male samples (true label 1), 72 were correctly predicted as male (true positive for class 1), while 55 were incorrectly classified as female (false negative for class 1).

These classification results can be partially accounted for by the descriptive morphometric feature statistics. From Table 4.1, female samples of *T. granosa* have more uniform and lower variance measurements than males, particularly in such features as shell length (SD = 7.49 for females vs. 31.75 for males). This reduced variability indicates that female samples constitute a closer group in feature space, thus are simpler for KNN to correctly classify. By comparison, the greater variation of male samples will most likely render them more spread out and vulnerable to overlap with female data. In addition, certain shape features (e.g., height, width, rib density) exhibit little variation between sexes and may thus make it more difficult for the model to differentiate between long male shells and curved female shells when the male values are closer to female means. These are some of the possible reasons why the model records a greater true positive value for females and false negatives for males.

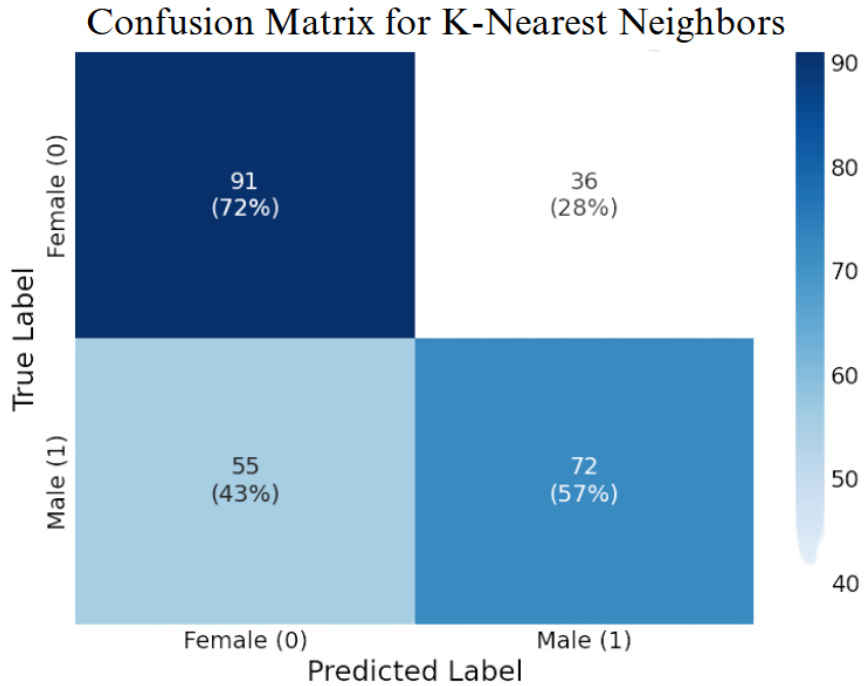


Figure 4.3: KNN confusion matrix for *T. granosa* sex classification.

Figure 4.4 displays the average receiver operating characteristic (ROC) curve, showing KNN’s ability to distinguish between positive and negative cases. The ROC curve helps assess the trade-off between sensitivity (true positive rate) and specificity (1 - false positive rate). The area under the curve (AUC) value, which ranges from 0.5 (random chance) to 1 (perfect discrimination), is used to evaluate the model’s overall performance. In this case, KNN achieved an average AUC of 0.7004, indicating that it performs better than random guessing and has reasonable predictive ability.

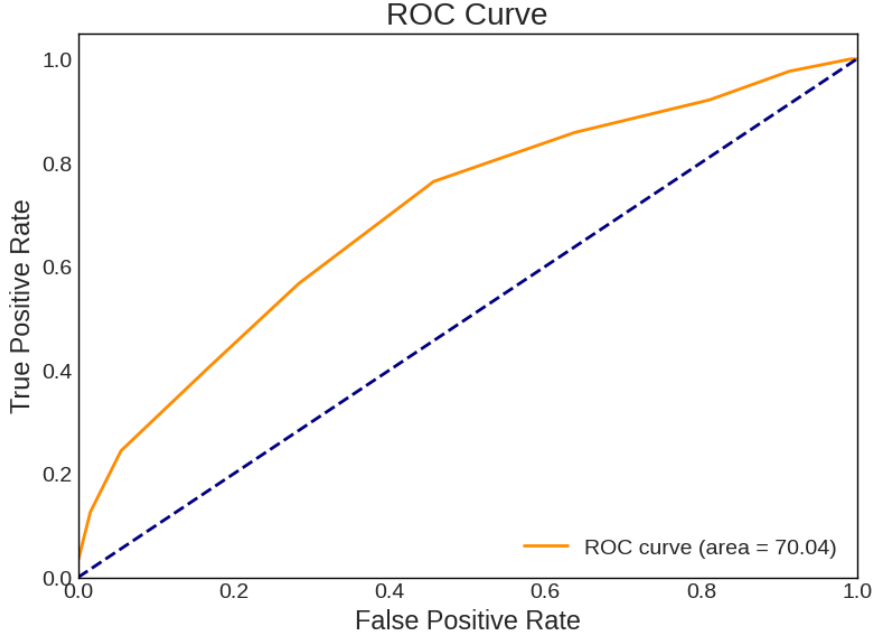


Figure 4.4: ROC curve with AUC score for KNN.

## 4.2 Deep Learning Analysis

This section presents the performance of the convolutional neural network (CNN) model in classifying the sex of *T. granosa* based on shell morphology. The analysis evaluates the model's ability to distinguish between male and female shell images using various evaluation metrics. This part of the paper includes six subsections: baseline model, comparison of individual and combined angles, training result and hyperparameter tuning, proposed model, learning rates and training behavior per fold, and visualizations for deep learning.

The machine learning analysis (*see Figure 4.4*) revealed that five of the original features produced significant results. The k-nearest neighbors (KNN) model achieved an accuracy of 64.16%, precision of 64.97%, recall of 64.16%, and an F1 Score of 63.75%. This section compares the model's performance across differ-

ent angles based on the results of the machine learning and feature importance analysis.

### 4.2.1 Baseline Model

This section presents the baseline model with a batch size of 16 and 20 epochs, which will serve as the starting point for comparison and provide a guideline for hyperparameter tuning. The focus will be on one of the angles, specifically the Left Lateral view, since the feature importance analysis using the Kruskal-Wallis Test indicated that the width-to-height ratio had the highest importance score, which is most visible from the Left Lateral view.

The unbalanced dataset, which consisted of 144 male samples and 127 female samples, achieved an accuracy of 65.27%, precision of 71.82%, recall of 58.99%, an F1 Score of 63.99%, an AUC score of 73.08%, and a loss of 0.6122. However, to address the class imbalance and enhance model performance, random undersampling was performed. This approach resulted in improved performance metrics for the balanced dataset, with an accuracy of 67.34%, precision of 69.43%, a recall of 64.06%, an F1 Score of 65.60%, an AUC score of 74.31%, and a lower loss of 0.5981.

Dataset	Accuracy (%)	Precision (%)	Recall (%)	F1 Score (%)	AUC score (%)	Loss
Imbalanced	65.27	71.82	58.99	63.99	73.08	0.6122
Balanced	67.34	69.43	64.06	65.60	74.31	0.5981

Table 4.5: Performance metrics for balanced vs imbalanced datasets (Batch Size: 16, Epochs: 20).

### 4.2.2 Comparison of Individual and Combined Angles

Using the same batch size and number of epochs, performance was compared across all individual angles and the combination of the two highest-performing angles based on accuracy, using a balanced dataset. For the combined analysis, samples from the two selected angles were placed side by side, and a new dataset folder was created for male and female samples.

Table 4.6 presents the performance metrics for each individual angle and the combination of the two highest-performing angles in terms of accuracy. The Left Lateral view achieved the highest accuracy (67.34%) and precision (69.43%), while the Dorsal view obtained the highest recall (77.88%) and F1 Score (69.96%). Meanwhile, the Ventral view recorded the highest AUC score (74.87%), indicating its strong ability to distinguish between classes. Combining the Ventral and Left Lateral views resulted in an overall accuracy of 62.60%, suggesting that while combined images may provide complementary information, individual angle views still outperformed the combined views under the current experimental setup.

Angle	Accuracy (%)	Precision (%)	Recall (%)	F1 Score (%)	AUC score (%)	Loss
Dorsal	66.54	63.76	77.88	69.96	73.09	0.6152
Ventral	67.30	69.33	66.18	66.53	74.87	0.6159
Anterior	51.57	31.11	6.31	10.02	65.87	0.6825
Posterior	61.43	63.48	51.17	54.25	70.12	0.6257
Left Lateral	67.34	69.43	64.06	65.60	74.31	0.5981
Right Lateral	65.37	67.18	59.82	62.99	71.02	0.6115
Ventral + Left Lateral	62.60	67.02	57.85	58.57	70.37	0.6433

Table 4.6: Performance metrics for individual and combined angles (Batch Size: 16, Epochs: 20).

### 4.2.3 Training Result and Hyperparameter Tuning

The Left Lateral angle view was selected for further optimization. Several experiments were conducted by tuning hyperparameters such as batch size, number of epochs, and activation functions. Each adjustment was compared against the baseline model to enhance performance and develop a robust CNN for sex classification of *T. granosa*.

The Left Lateral angle was chosen because it achieved the highest accuracy and precision among all individual views, and because the Kruskal-Wallis feature importance analysis indicated that the width-to-height ratio, a feature most visible from the lateral perspective, was the most significant morphological trait for classification. Therefore, focusing on this view was expected to maximize the model's learning capacity and improve classification performance.

#### A. Batch Size and Number of Epochs

Table 4.7 shows the results indicating that a batch size of 32 with 50 epochs achieved the best overall performance, with an accuracy of 71.68%, a precision of 72.52%, a recall of 69.29%, an F1 Score of 69.12%, and AUC score of 77.34%.

In contrast, increasing the batch size to 64 resulted in lower recall and F1 Scores, suggesting that smaller batch Sizes (16 or 32) are more effective for this dataset. A moderate batch size of 32 allowed the model to generalize better and maintain stable learning, while too large batch sizes may have led to underfitting.

Epoch	Batch Size	Accuracy (%)	Precision (%)	Recall (%)	F1 Score (%)	AUC Score (%)	Loss
20	16	67.34	69.43	64.06	65.60	74.31	0.5981
	32	68.13	72.25	58.95	62.34	74.76	0.6041
	64	56.71	65.96	36.83	41.46	71.28	0.6692
30	16	67.73	70.17	64.06	65.72	75.76	0.5900
	32	71.28	73.17	66.89	68.27	76.76	0.5832
	64	57.95	61.94	48.12	52.66	71.22	0.6241
50	16	67.73	70.17	64.06	65.72	75.76	0.5900
	32	71.68	72.52	69.29	69.12	77.34	0.5824
	64	61.10	62.68	56.12	56.83	73.46	0.6086

Table 4.7: Effect of batch size and epoch values on CNN model performance.

## B. Activation Functions

Table 4.8 shows the performance of different activation functions applied to the CNN model trained with a batch size of 32 and 50 epochs. Based on the results, the ReLU activation function achieved the best overall performance, with an accuracy of 71.68%, precision of 72.52%, recall of 69.29%, F1 Score of 69.12%, and AUC score of 77.34%, along with the lowest loss at 0.5824. This suggests that ReLU remains an effective activation function for the classification of *T. granosa*, outperforming both ELU and PReLU in this setup.

Activation Functions	Accuracy (%)	Precision (%)	Recall (%)	F1 Score (%)	AUC score (%)	Loss
ReLU	71.68	72.52	69.29	69.12	77.34	0.5824
ELU	53.14	32.91	53.08	39.95	58.23	0.6796
PreLU	62.64	66.59	50.43	56.96	72.33	0.6162

Table 4.8: Performance metrics for different activation functions (Batch Size: 32, Epochs: 50).

### 4.2.4 Proposed Model

This section presents the performance evaluation of the proposed convolutional neural network (CNN) model, trained with a batch size of 32, 50 epochs, and using the ReLU activation function. The model's effectiveness was assessed through 5-fold cross-validation to ensure robustness and generalizability across different data

partitions.

The proposed model consistently achieved high performance in Folds 1, 3, and 5, with accuracy above 76%, and strong recall and AUC scores, demonstrating its potential for reliable sex identification of *T. granosa*. The mean standard deviation for the performance metrics is  $71.68 \pm 7.32$  for accuracy,  $71.68 \pm 7.32$  for precision,  $72.52 \pm 0.02$  for recall,  $72.52 \pm 0.02$  for F1 score, and  $69.29 \pm 0.22$  for AUC score. The standard deviation indicates the spread and variability in the performance. All metrics show a good indication of spread and consistency across folds. However, some with higher standard deviation values are recall, and F1 score indicates some inconsistencies in predicting positive classes across the folds.

The slight variation in performance across folds may be attributed to differences in data distribution, emphasizing the importance of further data augmentation and balancing for future work.

Fold no.	Accuracy (%)	Precision (%)	Recall (%)	F1 Score (%)	AUC score (%)	Loss
Fold 1	76.47	70.59	92.31	80.00	73.08	0.5975
Fold 2	62.75	70.59	46.15	55.81	71.85	0.6202
Fold 3	78.43	75.00	84.00	79.25	84.92	0.5392
Fold 4	62.75	71.43	40.00	51.28	71.08	0.6331
Fold 5	78.00	75.00	84.00	79.25	85.76	0.5219
Mean $\pm$ SD	$71.68 \pm 7.32$	$72.52 \pm 2.05$	$69.29 \pm 21.71$	$69.12 \pm 12.80$	$77.34 \pm 6.57$	$0.5824 \pm 0.04$

Table 4.9: Per-fold performance metrics (Batch Size: 32, Epochs: 50, Activation Function: ReLU) and corresponding mean and standard deviation.

#### 4.2.5 Learning Rates and Training Behavior per Fold

This section presents the learning rate adjustments, early stopping events, and best epoch selections for each fold during the 5-fold cross-validation of the proposed model. During training, the ReduceLROnPlateau callback was employed

to monitor the validation loss and automatically reduce the learning rate when performance plateaued. Additionally, EarlyStopping was utilized to halt training once no further improvement was observed after a set patience, and the model weights were restored from the end of the best-performing epoch to ensure optimal performance.

The following table summarizes the epochs where learning rate reductions occurred, the adjusted learning rates, the epochs at which early stopping took place, and the best epochs from which model weights were restored for each fold.

Fold no.	Epoch (LR Reduced)	Learning Rate After Reduction	Early Stopping Epoch	Best Epoch (Restored)
Fold 1	20	0.0005000	25	17
	23	0.0002500		
Fold 2	9	0.0005000	19	11
	14	0.0002500		
	17	0.0001250		
Fold 3	15	0.0005000	20	12
	18	0.0002500		
Fold 4	12	0.0005000	32	24
	15	0.0002500		
	27	0.0001250		
	30	0.0000625		
Fold 5	20	0.0005000	25	17
	23	0.0002500		

Table 4.10: Learning rate reductions, early stopping, and best epochs per fold during 5-fold cross-validation.

#### 4.2.6 Visualizations for Deep Learning

Figure 4.5 shows the performance of the model in the training and validation in terms of accuracy across five folds. The graph across folds displays a consistent upward trend for the training accuracy. However, there is an observable change in

the performance, particularly in Folds 1 and 2, where it shows a slight downward trend in the validation accuracy.

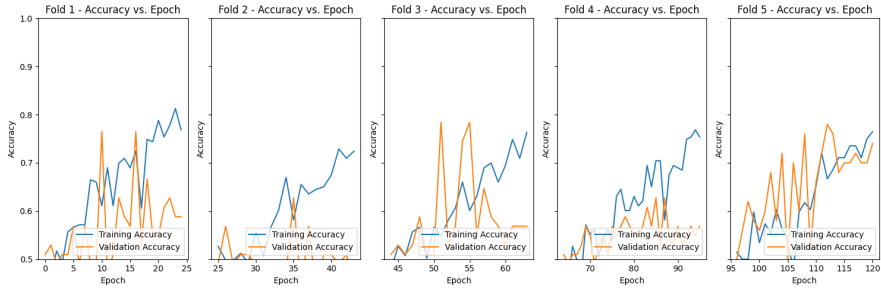


Figure 4.5: Training and validation accuracy per fold.

Figure 4.6 shows the average performance of the model in terms of training and validation accuracy across five folds. An upward trend is observable in the training and validation accuracy, indicating that the model gradually improves over the epochs. While fluctuations or dips can be seen in the validation accuracy, the model recovers in later epochs. The training accuracy remains consistently higher than the validation accuracy, which is expected behavior, as it learns from the training data. Generally, the model demonstrates a gradual improvement in learning, as reflected in the average upward trend aggregated across five folds.

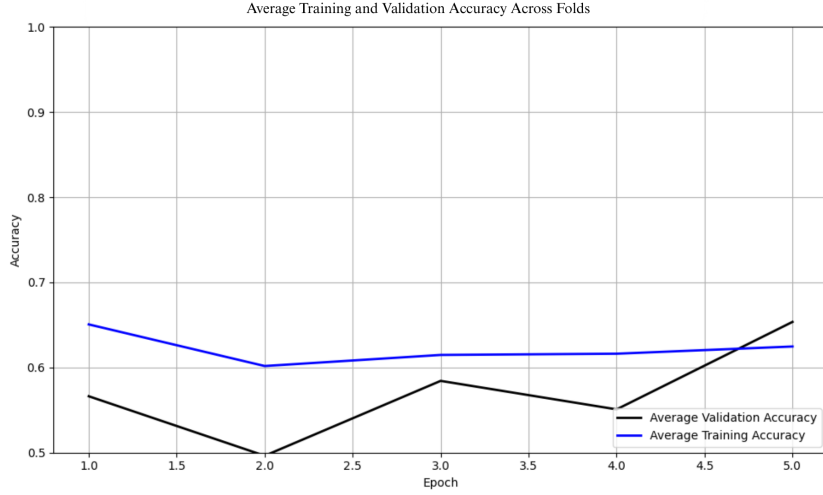


Figure 4.6: Average training and validation accuracy across folds.

Figure 4.7 shows the performance of the model in the training and validation in terms of the training and validation loss across five folds. The graph across folds displays a consistent downward trend for the training loss. On the other hand, there is an observable change in the performance, especially in Folds 1,2,3, and 4, where it shows an upward trend in the validation loss. This is an implication for the learning performance of the model, as it may not be learning effectively.

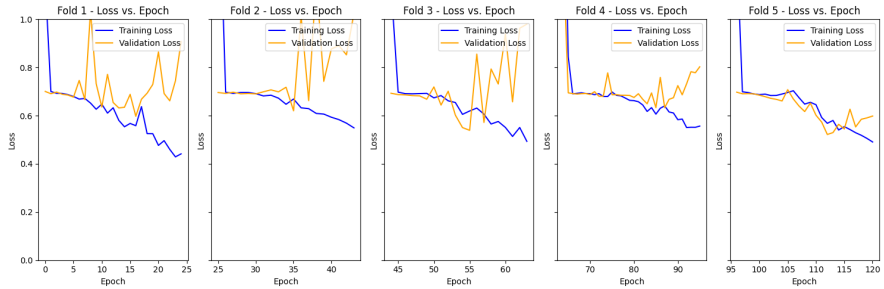


Figure 4.7: Training and validation loss per fold.

Figure 4.8 shows the average performance of the model regarding training and validation loss across five folds. A continuous downward trend is observed in training and validation accuracy, indicating that the model's loss gradually de-

creases across epochs. This suggests that the model generalizes better following the initial instability in the earlier epoch in the folds. Additionally, the training loss consistently remains lower than the validation loss, since the model was directly optimized on the training set. Overall, the downward trend in training and validation loss signifies that the model is learning and improving across the five folds.

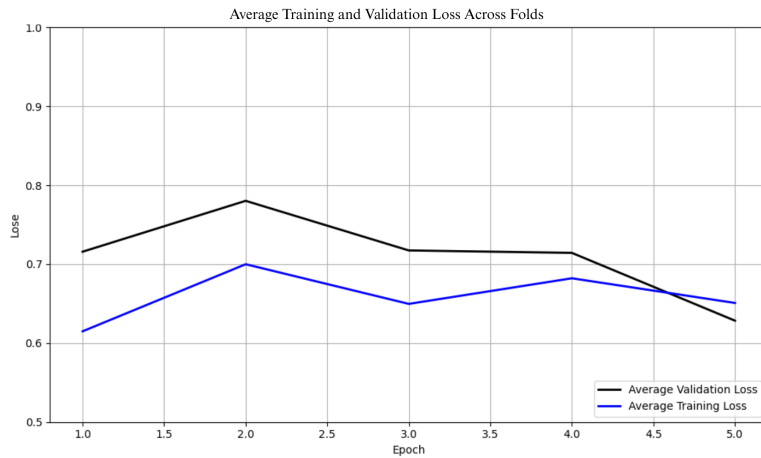


Figure 4.8: Average training and validation loss across folds.

Figure 4.9 shows the confusion matrix for the true class label and predicted class label after the training and validation. The matrix shows the correctly predicted male and female samples and their corresponding percentages. Females have slightly higher true positives compared to males in the number and percentages, which are 94 and 88, corresponding to 74% and 69%, respectively. Additionally, the falsely classified samples were 33 for females and 39 for males, respectively, accounting for 26% and 31%.

The results from the confusion matrix of the CNN model also matches what is observed in the descriptive statistics. Just like in the results from KNN, female

samples again have slightly better correct classification rates. This can be explained by having lower variability in their morphometric attributes—particularly shell length, with females having a much smaller standard deviation ( $SD = 7.49$ ) than males ( $SD = 31.75$ ). This similarity probably makes the female class simpler to acquire and generalize for the model. Additionally, some shape-based ratios (for instance, UL ratio, UH ratio) that varied subtly but consistently by sex might provide sharper decision boundaries for females, particularly if the neural network is sensitive to subtle differences in spatial features. In contrast, the larger variation of male feature values may have caused intersections with female patterns and thus raised the rate of false negatives among males. This implies that although the deep learning model captures complex patterns, variability in features remains a source of error for reliable classification of the male class.

Confusion Matrix for Convolutional Neural Network

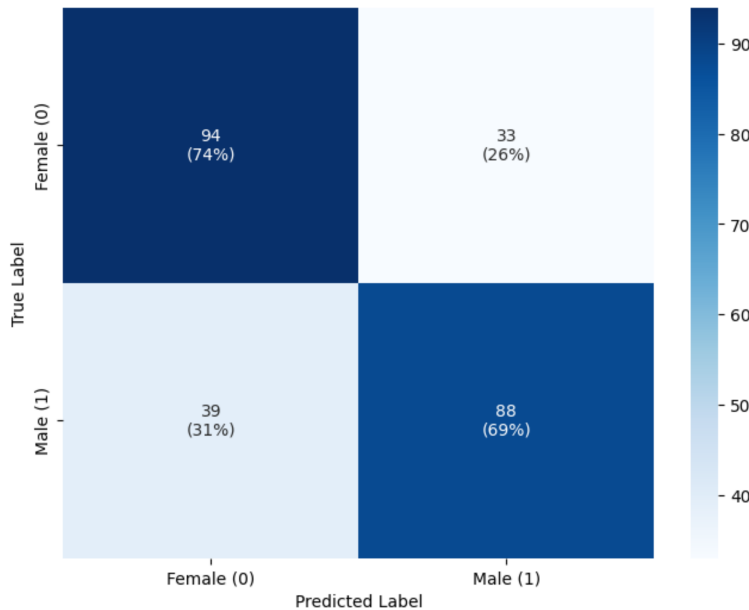


Figure 4.9: Confusion matrix for CNN model (Batch Size: 32, Epochs: 50, Activation Function: ReLU).

Figure 4.10 shows the average receiver operating characteristic (ROC) curve, showing the proposed model’s ability to correctly identify the true positives, which can help determine the trade-off between specificity and sensitivity. It will also determine the model’s validity, supporting that it is not being predicted based only on random chance. The range of area under the receiver operating characteristic curve (AUC-ROC) is between 0.5 and 1. The model achieved an average score of 0.7734, which is better than random chance and a positive indication that the model is performing reasonably.

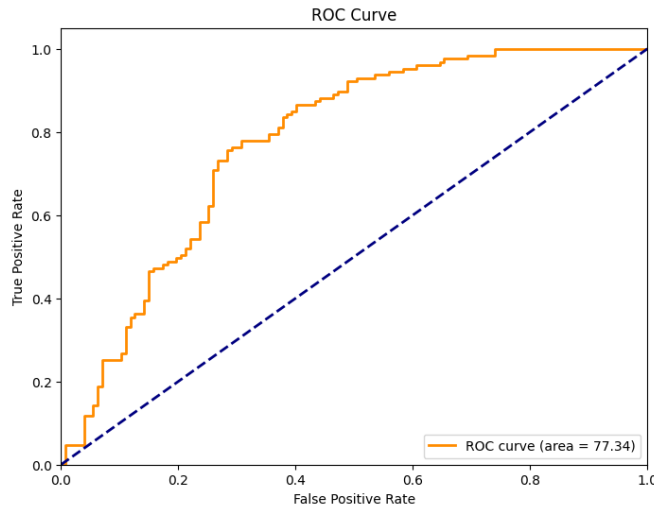


Figure 4.10: ROC curve with area under the curve (AUC) score for the proposed model.

### 4.3 Discussions

This study aimed to develop a noninvasive method for identifying the sex of *T. granosa* using machine learning and deep learning technologies. Specifically, it explored the relevance of linear shell measurements and image data in building accurate classification models that can support sustainable aquaculture practices.

In the machine learning experiments, feature selection played a key role in enhancing model performance. A reduced set of five statistically significant features, which were identified through Mann-Whitney U and Kruskal-Wallis tests, outperformed models using all available features. The k-nearest neighbors (KNN) classifier, trained on these five features, achieved an accuracy of 64.16%, precision of 64.97%, recall of 64.16%, F1 score of 63.57%, and an AUC-ROC score of 70.04%. The width-height ratio observed from the left lateral view emerged as the most discriminative feature, with a correlation score of  $p = 0.18$ .

Deep learning experiments further revealed the impact of image angle and hyper-parameter tuning on classification performance. The left lateral view consistently yielded the highest metrics, with the best model reaching 71.68% accuracy, 72.52% precision, 69.29% recall, 69.12% F1 score, and 77.34% AUC using a batch size of 32 and 50 training epochs. Additionally, balanced dataset and activation function contributed to improved model performance.

The improved accuracy from models using fewer, more relevant features supports the idea that dimensionality reduction, when guided by statistical analysis, can enhance classification. The prominence of the left lateral view in both machine learning and deep learning results suggests that this angle reveals key morpho-

logical traits tied to sex differentiation. This aligns with the biological premise that some external characteristics may be more distinguishable when viewed from specific perspectives.

These findings demonstrate the feasibility of a noninvasive, accurate, and scalable approach to sex identification in *T. granosa*. This is especially important in aquaculture, where traditional sex identification methods are often invasive or require specialized knowledge. By reducing the need for physical intervention, this approach promotes animal welfare and operational efficiency, potentially enabling real-time sex identification in aquaculture settings.

When compared to related work, such as the gender classification of Chinese mitten crabs using CNNs (Cui et al., 2020), this study reflects both shared methodologies and important distinctions. While both utilized CNN architectures, differences in image resolution, dataset characteristics, and species-specific morphology may explain the performance gap which is 98.90% in the crab study compared to 71.68% in this study. The lower accuracy here likely reflects subtler morphological differences in *T. granosa* and limited dataset size.

Despite promising results, the study has several limitations. The dataset size (271 samples) was relatively small, which may have affected model generalizability. Additionally, image data was constrained to six fixed angles, potentially missing other informative views. These limitations may restrict the model's effectiveness across diverse populations or environmental conditions.



# Chapter 5

## Conclusion and Recommendations

### 5.1 Conclusion

This study aimed to develop a noninvasive approach for sex identification of *Tegillarca granosa* using morphometric and morphological characteristics through the integration of machine learning and deep learning technologies. In particular, it sought to determine whether measurable shell features and image-based characteristics could reliably distinguish between male and female blood cockles.

The findings support the feasibility of this approach, with the proposed CNN model achieving a classification accuracy of 71.68%. This performance demonstrates that linear morphological and features, when processed through deep learning, can serve as reliable indicators of sex in *T. granosa*. In comparison to traditional, more invasive methods such as dissection or spawning observation,

this method presents a promising alternative that could be useful in aquaculture operations requiring rapid and non-destructive sex identification.

The study also contributes a manually curated dataset of labeled images and shell measurements, which can serve as a foundation for further studies in this underexplored domain. By emphasizing noninvasiveness, the research addresses a crucial need in sustainable aquaculture practices, particularly in improving broodstock selection without harming specimens.

Although challenges such as limited sample size and computing resources were encountered, the overall results suggest that machine learning and deep learning techniques offer a scalable and practical solution for this biological classification task. As such, the study lays the groundwork for future research to expand the dataset, explore more advanced neural architectures, and develop real-time sex identification systems suitable for field or hatchery deployment.

## 5.2 Recommendations

This special problem aims to serve as a foundational study for future work involving the application of machine learning and deep learning in aquaculture. Given the importance of accurate sex identification for breeding and stock management, several recommendations are proposed to enhance future studies.

Future work should consider incorporating shape analysis and exploring more advanced deep learning architectures, such as ResNet, SqueezeNet, and Inception-Net. The use of transfer learning may also enhance classification performance, especially when working with limited datasets. Additionally, real-time sex identi-

fication could be achieved by developing a system that captures rotational views of the shell from dorsal, lateral, and anterior angles.

Analyzing the specific morphological features that contributed to the success or failure of the model’s predictions can also improve the model performance. This includes identifying combinations of morphological features that lead to accurate classifications, as well as those that result in misclassification. Furthermore, examining which morphological traits correlate strongly with prediction accuracy may offer deeper insights into sexual dimorphism in *T. granosa*.

Due to time constraints, this study utilized a dataset of 1,626 images, with 271 images per angle. Increasing the number and diversity of samples can help improve model generalization and robustness. Expanding the dataset to include different populations and environmental contexts would provide a more comprehensive understanding of morphological variation in *T. granosa*. Instead of manually gathering the linear measurements, another area of exploration is the automated collection of measurements using images.

To ensure consistency and data quality, future researchers are encouraged to establish a more controlled image acquisition environment, using a green or neutral background, consistent lighting, and fixed camera positioning. Image processing techniques, including morphological transformations or background removal, should be refined to highlight relevant features and enhance model accuracy.

Since this study was conducted in a controlled environment, future researchers should focus on developing deployable, practical applications for real-life aquaculture settings, such as creating a user-friendly mobile application with real-time sex classification.

The dataset produced in this study may serve as a valuable resource for future research in deep learning and marine biology. It can be further analyzed using advanced techniques to uncover patterns of sexual dimorphism and develop scalable, real-time applications for aquaculture settings.

# Chapter 6

## References

- Adams, D. C., Rohlf, F. J., & Slice, D. E. (2004). Geometric morphometrics: ten years of progress following the ‘revolution’. *Italian Journal of Zoology*, *71*, 5–16. doi: 10.1080/11250000409356545
- Afiati, N. (2007, 01). Gonad maturation of two intertidal blood clams *Anadara granosa* (l.) and *Anadara antiquata* (l.) (bivalvia: Arcidae) in central java. *10*.
- Aji, L. P. (2011). Review: Spawning induction in bivalve. *Jurnal Penelitian Sains*, *14*.
- Arifin, W. A., Ariawan, I., Rosalia, A. A., Lukman, L., & Tufailah, N. (2021). Data scaling performance on various machine learning algorithms to identify abalone sex. *Jurnal Teknologi Dan Sistem Komputer*, *10*(1), 26–31. doi: 10.14710/jtsiskom.2021.14105
- Arkhipkin, A. I. (2005). Statoliths as ‘black boxes’ (life recorders) in squid. *Marine and Freshwater Research*, *56*, 573–583. doi: 10.1071/mf04158
- Awan, A. A. (2022, November). *A complete guide to data augmentation*.

- tion. Retrieved from <https://www.datacamp.com/tutorial/complete-guide-data-augmentation>
- Aypa, S. M., & Baconguis, S. R. (2000). Philippines: Mangrove-friendly aquaculture. In J. H. Primavera, L. M. B. Garcia, M. T. Castaños, & M. B. Surtida (Eds.), *Mangrove-friendly aquaculture: Proceedings of the workshop on mangrove-friendly aquaculture organized by the SEAFDEC aquaculture department, january 11-15, 1999, Iloilo City, Philippines* (pp. 41–56).
- BFAR. (2019). *Philippine fisheries profile 2018* (Tech. Rep.). PCA Compound, Elliptical Road, Quezon City, Philippines: Bureau of Fisheries and Aquatic Resources.
- Boey, P.-L., Maniam, G. P., Hamid, S. A., & Ali, D. M. H. (2011). Utilization of waste cockle shell (*Anadara granosa*) in biodiesel production from palm olein: Optimization using response surface methodology. *Fuel*, 90(7), 2353–2358. doi: 10.1016/j.fuel.2011.03.002
- Breton, S., Capt, C., Guerra, D., & Stewart, D. (2017, June). *Sex determining mechanisms in bivalves*. Preprints.org. doi: 10.20944/preprints201706.0127.v1
- Breton, S., Stewart, D. T., Shepardson, S., Trdan, R. J., Bogan, A. E., Chapman, E. G., ... Hoeh, W. R. (2010). Novel protein genes in animal mtDNA: A new sex determination system in freshwater mussels (bivalvia: Unionoida)? *Molecular Biology and Evolution*, 28(5), 1645–1659. doi: 10.1093/molbev/msq345
- Budd, A., Banh, Q., Domingos, J., & Jerry, D. (2015). Sex control in fish: Approaches, challenges and opportunities for aquaculture. *Journal of Marine Science and Engineering*, 3(2), 329–355. doi: 10.3390/jmse3020329
- Burdon, D., Callaway, R., Elliott, M., Smith, T., & Wither, A. (2014, 04).

- Mass mortalities in bivalve populations: A review of the edible cockle *Cerastoderma edule* (l.). *Estuarine, Coastal and Shelf Science*, 150. doi: 10.1016/j.ecss.2014.04.011
- Campos, A., Tedesco, S., Vasconcelos, V., & Cristobal, S. (2012). Proteomic research in bivalves: Towards the identification of molecular markers of aquatic pollution. *Proteomic Research in Bivalves*, 75(14), 4346–4359. doi: 10.1016/j.jprot.2012.04.027
- Cerqueira, V., Santos, M., Baghoussi, Y., & Soares, C. (2024). On-the-fly data augmentation for forecasting with deep learning. *ArXiv (Cornell University)*. Retrieved from <https://doi.org/10.48550/arxiv.2404.16918>
- Coe, W. R. (1943). Sexual differentiation in mollusks. i. pelecypods. *The Quarterly Review of Biology*, 18, 154–164. doi: 10.1086/qrb.1943.18.issue-2
- Collin, R. (2013). Phylogenetic patterns and phenotypic plasticity of molluscan sexual systems. *Integrative and Comparative Biology*, 53, 723–735. doi: 10.1093/icb/icb076
- Concepcion, R., Guillermo, M., Tanner, S. E., Fonseca, V., & Duarte, B. (2023). Bivalvenet: A hybrid deep neural network for common cockle (*Cerastoderma edule*) geographical traceability based on shell image analysis. *Ecological Informatics*, 78, 102344. doi: 10.1016/j.ecoinf.2023.102344
- Cui, Y., Pan, T., Chen, S., & Zou, X. (2020). A gender classification method for chinese mitten crab using deep convolutional neural network. *Multi-media Tools and Applications*, 79(11-12), 7669–7684. doi: <https://doi.org/10.1007/s11042-019-08355-w>
- Davenport, J., & Wong, T. (1986, September). Responses of the blood cockle *Anadara granosa* (l.) (bivalvia: Arcidae) to salinity, hypoxia and aerial exposure. *Aquaculture*, 56(2), 151–162. Retrieved from <https://doi.org/>

- 10.1016/0044-8486(86)90024-4 doi: 10.1016/0044-8486(86)90024-4
- Doering, P., & Ludwig, J. (1990). Shape analysis of otoliths—a tool for indirect ageing of eel, *Anguilla anguilla* (L.)? *International Review of Hydrobiology*, 75(6), 737–743. doi: 10.1002/iroh.19900750607
- Erica, D. (2018, April 4). *Clam dissection: A first step into dissection and anatomy for young learners*. Rosie Research. Retrieved from <https://rosieresearch.com/clam-dissection-anatomy/>
- Fao 2024 report: Sustainable aquatic food systems important for global food security – european fishmeal. (2024). <https://effop.org/news-events/fao-2024-report-sustainable-aquatic-food-systems-important-for-global-food-security/>.
- Ferguson, G. J., Ward, T. M., & Gillanders, B. M. (2011). Otolith shape and elemental composition: Complementary tools for stock discrimination of mulloway (*Argyrosomus japonicus*) in southern australia. *Fish Research*, 110, 75–83. doi: 10.1016/j.fishres.2011.03.014
- GeeksforGeeks. (2020, August 6). Stratified k fold cross validation. Retrieved from <https://www.geeksforgeeks.org/stratified-k-fold-cross-validation/>
- GeeksforGeeks. (2024, May). Cross-validation using k-fold with scikit-learn. Retrieved from <https://www.geeksforgeeks.org/cross-validation-using-k-fold-with-scikit-learn/> (Accessed: 2025-04-23)
- Gosling, E. (2004). *Bivalve molluscs: biology, ecology and culture*. Oxford: Blackwell Science.
- Heller, J. (1993). Hermaphroditism in molluscs. *Biological Journal of the Linnean Society*, 48, 19–42. doi: 10.1111/bij.1993.48.issue-1
- Hussain, S. S., & Zaidi, S. S. H. (2024). Adaboost ensemble approach with

- weak classifiers for gear fault diagnosis and prognosis in dc motors. *Applied Sciences*, 14(7), 3105. doi: 10.3390/app14073105
- Ishak, A. R., Mohamad, S., Soo, T. K., & Hamid, F. S. (2016). Leachate and surface water characterization and heavy metal health risk on cockles in kuala selangor. In *Procedia - social and behavioral sciences* (Vol. 222, pp. 263–271). doi: 10.1016/j.sbspro.2016.05.156
- Jaiswal, S. (2024, January 4). *What is normalization in machine learning? a comprehensive guide to data rescaling*. DataCamp. Retrieved from <https://www.datacamp.com/tutorial/normalization-in-machine-learning> (Accessed 2025-04-23)
- Karapunar, B., Werner, W., Fürsich, F. T., & Nützel, A. (2021). The earliest example of sexual dimorphism in bivalves—evidence from the astartid *Nicanella* (lower jurassic, southern germany). *Journal of Paleontology*, 95(6), 1216–1225. doi: 10.1017/jpa.2021.48
- Kerr, L. A., & Campana, S. E. (2014). Chemical composition of fish hard parts as a natural marker of fish stocks. In *Stock identification methods* (pp. 205–234). Elsevier. doi: 10.1016/b978-0-12-397003-9.00011-4
- Kim, E., Yang, S.-M., Cha, J.-E., Jung, D.-H., & Kim, H.-Y. (2024). Deep learning-based phenotype classification of three ark shells: *Anadara kagoshimensis*, *Tegillarca granosa*, and *Anadara Broughtonii*. *Frontiers in Marine Science*, 11. doi: 10.3389/fmars.2024.1356356
- Lee, J. H. (1997). Studies on the gonadal development and gametogenesis of the granulated ark, *Tegillarca granosa* (linne). *The Korean Journal of Malacology*, 13, 55–64.
- Leguá, J., Plaza, G., Pérez, D., & Arkhipkin, A. (2013). Otolith shape analysis as a tool for stock identification of the southern blue whiting, *Micromesistius*

- australis*. *Latin American Journal of Aquatic Research*, 41, 479–489.
- Mahé, K., Oudard, C., Mille, T., Keating, J., Gonçalves, P., Clausen, L. W., & et al. (2016). Identifying blue whiting (*Micromesistius poutassou*) stock structure in the northeast atlantic by otolith shape analysis. *Canadian Journal of Fisheries and Aquatic Sciences*, 73, 1363–1371. doi: 10.1139/cjfas-2015-0332
- May, K., Maung, C., Phy, E., & Tun, N. (2021). Spawning period of blood cockle *Tegillarca granosa* (linnaeus, 1758) in myeik coastal areas. *J. Myanmar Acad. Arts Sci*, 4.
- Miranda, D. V., & Ferriols, V. M. E. N. (2023). Initial attempts on spawning and larval rearing of the blood cockle, *Tegillarca granosa* (linnaeus, 1758), in the philippines. *Asian Fisheries Science*, 36(2). doi: 10.33997/j.afs.2023.36.2.001
- Mérigot, B., Letourneur, Y., & Lecomte-Finiger, R. (2007). Characterization of local populations of the common sole *solea solea* (pisces, soleidae) in the nw mediterranean through otolith morphometrics and shape analysis. *Marine Biology*, 151(3), 997–1008. doi: 10.1007/s00227-006-0549-0
- Nahm, F. S. (2022). Receiver operating characteristic curve: Overview and practical use for clinicians. *Korean Journal of Anesthesiology*, 75(1), 25–36. Retrieved from <https://doi.org/10.4097/kja.21209> doi: 10.4097/kja.21209
- Narasimham, K. A. (1988). Taxonomy of the blood clams anadara (*Tegillarca granosa* (linnaeus, 1758) and a. (t.) rhombea (born, 1780).
- Naylor, R. L., Goldburg, R. J., Primavera, J. H., Kautsky, N., Beveridge, M. C. M., Clay, J., ... Troell, M. (2000). Effect of aquaculture on world fish supplies. *Nature*, 405(6790), 1017–1024. doi: 10.1038/35016500

- Ponton, D. (2006). Is geometric morphometrics efficient for comparing otolith shape of different fish species? *Journal of Morphology*, 267(7), 750–757. doi: 10.1002/jmor.10439
- Quenu, M., Trewick, S. A., Brescia, F., & Morgan-Richards, M. (2020). Geometric morphometrics and machine learning challenge currently accepted species limits of the land snail *placostylus* (pulmonata: Bothriembryontidae) on the isle of pines, new caledonia. *Journal of Molluscan Studies*, 86(1), 35–41. doi: 10.1093/mollus/eyz031
- Ribeiro, D. (2024, Aug). *Diogo ribeiro. data science. kruskal-wallis test.* Retrieved from [https://diogoribeiro7.github.io/statistics/data%20analysis/kruskal\\_wallis/](https://diogoribeiro7.github.io/statistics/data%20analysis/kruskal_wallis/) (Accessed: 2025-04-23)
- Sany, S. B. T., Hashim, R., Rezayi, M., Salleh, A., Rahman, M. A., Safari, O., & Sasekumar, A. (2014). Human health risk of polycyclic aromatic hydrocarbons from consumption of blood cockle and exposure to contaminated sediments and water along the klang strait, malaysia. *Marine Pollution Bulletin*, 84(1-2), 268–279. doi: 10.1016/j.marpolbul.2014.05.004
- Srisunont, C., Nobpakhun, Y., Yamalee, C., & Srisunont, T. (2020). Influence of seasonal variation and anthropogenic stress on blood cockle (*Tegillarca Granosa*) production potential. *Influence of Seasonal Variation and Anthropogenic Stress on Blood Cockle (Tegillarca Granosa) Production Potential*, 44(2), 62–82.
- Tarca, A. L., Carey, V. J., Chen, X.-w., Romero, R., & Drăghici, S. (2007). Machine learning and its applications to biology. *PLoS Computational Biology*, 3(6), e116. doi: 10.1371/journal.pcbi.0030116
- Team, K. (n.d.). *Keras documentation: Reducelronplateau.* Retrieved from [https://keras.io/api/callbacks/reduce\\_lr\\_on\\_plateau/](https://keras.io/api/callbacks/reduce_lr_on_plateau/)

- Thompson, R. J., Newell, R. I. E., Kennedy, V. S., & Mann, R. (1996). Reproductive process and early development. In V. S. Kennedy, R. I. E. Newell, & A. F. Eble (Eds.), *The eastern oyster crassostrea virginica* (pp. 335–370). College Park, MD: Maryland Sea Grant.
- Tsutsumi, M., Saito, N., Koyabu, D., & Furusawa, C. (2023). A deep learning approach for morphological feature extraction based on variational auto-encoder: An application to mandible shape. *Npj Systems Biology and Applications*, 9(1), 1–12. doi: 10.1038/s41540-023-00293-6
- Wong, T. M., & Lim, T. G. (2018). *Cockle (Anadara granosa) seed produced in the laboratory, malaysia*. (Handle.net) doi: 10.3366/in\_3366.pdf
- Zahn, C. T., & Roskies, R. Z. (1972). Fourier descriptors for plane closed curves. *IEEE Transactions on Computers*, C-21, 269–281. doi: 10.1109/tc.1972.5008949
- Zelditch, M., Swiderski, D. L., & Sheets, H. D. (2004). *Geometric morphometrics for biologists: A primer* (2nd ed.). Waltham: Elsevier Academic Press.
- Zha, S., Tang, Y., Shi, W., Liu, H., Sun, C., Bao, Y., & Liu, G. (2022). Impacts of four commonly used nanoparticles on the metabolism of a marine bivalve species, *Tegillarca granosa*. *Chemosphere*, 296, 134079. doi: 10.1016/j.chemosphere.2022.134079
- Zhan, P. L., Zha, & Bao, Y. (2022). Hypoxia-mediated immunotoxicity in the blood clam *Tegillarca granosa*. *Marine Environmental Research*, 177. Retrieved from <https://doi.org/10.1016/j.marenvres.2022.105632>

# Appendix A

## Code Snippets

### i. Machine Learning

This section displays the key steps in the machine learning analysis by performing feature engineering to create and transform a new dataset, identifying the most significant features through the Kruskal-Wallis Test, applying random undersampling to address the minimal imbalance in the dataset, and conducting five-fold cross-validation to evaluate the model's performance.

```
female_litob['LW_ratio']= female_litob['Length'] / female_litob['Width']
female_litob['LH_ratio'] = female_litob['Length'] / female_litob['Height']
female_litob['WH_ratio'] = female_litob['Width'] / female_litob['Height']
# female_litob['DU_ratio'] = female_litob['Distance Umbos'] / female_litob['Height']
female_litob['UL_ratio'] = female_litob['Distance Umbos'] / female_litob['Length']
female_litob['HL_ratio'] = female_litob['Length (Hinge Line)'] / female_litob['Length']
female_litob['UH_ratio'] = female_litob['Distance Umbos'] / female_litob['Height']
female_litob['Rib Density'] = female_litob['Rib count'] / female_litob['Length']
```

Figure A.1: Feature engineering used to create and transform the dataset for machine learning analysis.

```

sorted_features = feature_importance_scores.sort_values(ascending=False)
colors = sns.color_palette("Blues_d", len(sorted_features))
colors = colors[::-1]
plt.figure(figsize=(10, 6))

# Map codenames to sorted_features.index
sorted_features.index = sorted_features.index.map(codenames)

sns.barplot(x=sorted_features.values, y=sorted_features.index, hue = sorted_features.index, palette=colors,dodge=False,leg
plt.xlabel("Kruskal-Wallis Statistic")
plt.ylabel("Features")
plt.title("Feature Importance based on Kruskal-Wallis Test")
plt.show()

```

Figure A.2: Feature importance scores derived from the Kruskal-Wallis test to identify the most significant variables.

```

from imblearn.under_sampling import RandomUnderSampler

rus = RandomUnderSampler(sampling_strategy=1) # Numerical value
# rus = RandomUnderSampler(sampling_strategy="not minority") # String
X_res, y_res = rus.fit_resample(X, y)

ax = y_res.value_counts().plot.pie(autopct='%.2f')
_ = ax.set_title("Under-sampling")

```

Figure A.3: Random undersampling applied in machine learning to address class imbalance.

## ii. Image Processing

This section displays the key steps in the image processing by resizing the images to have similar dimensions of 256x256, and the shadows were removed to improve the image quality, and remove noise before proceeding to the deep learning operations.

```

for model_name, (model, param_grid) in models_and_grids.items():
    print(f"Training {model_name}...")
    grid_search = GridSearchCV(estimator=model, param_grid=param_grid, cv=5, scoring='accuracy', return_train_score=False,
                               grid_search.fit(X, y)

    # Get the best estimator's CV results
    best_index = grid_search.best_index_

    # Get fold scores for the best parameters only
    fold_scores = [
        grid_search.cv_results_['split0_test_score'][best_index],
        grid_search.cv_results_['split1_test_score'][best_index],
        grid_search.cv_results_['split2_test_score'][best_index],
        grid_search.cv_results_['split3_test_score'][best_index],
        grid_search.cv_results_['split4_test_score'][best_index]
    ]

    # Calculate the average score across folds
    avg_score = sum(fold_scores) / len(fold_scores)

    # Convert to percentage by multiplying by 100 for display
    fold_scores_percentage = [score * 100 for score in fold_scores]
    avg_score_percentage = avg_score * 100

    # Round each fold score individually
    fold_scores_rounded = [round(score, 2) for score in fold_scores_percentage]

    # Round the average score
    avg_score_rounded = round(avg_score_percentage, 2)

    # Append the fold scores and average score to the list
    model_scores.append({
        'Model': model_name,
        'Fold 1': fold_scores_rounded[0],
        'Fold 2': fold_scores_rounded[1],
        'Fold 3': fold_scores_rounded[2],
        'Fold 4': fold_scores_rounded[3],
        'Fold 5': fold_scores_rounded[4],
        'Average CV Score': avg_score_rounded,
        'Best Parameters': grid_search.best_params_
    })
)

```

Figure A.4: Five-fold cross-validation used to evaluate and tune machine learning model performance.

```

# Process each image
for img_name in image_files:
    img_path = os.path.join(input_male, img_name)
    output_path = os.path.join(output_male, img_name)

    # Read the image
    image = cv2.imread(img_path)
    if image is None:
        print(f"Skipping invalid image: {img_path}")
        continue

    # Resize and pad the image to 256x256
    resized_image = resize_and_pad(image, 256)

```

Figure A.5: Resizing images to 256x256 pixels for consistent input dimensions.

```

# Convert to HSV and apply threshold
frame_HSV = cv.cvtColor(frame, cv.COLOR_BGR2HSV)
frame_threshold = cv.inRange(frame_HSV, (low_H, low_S, low_V), (high_H, high_S, high_V))

# Filling holes
im_floodfill = frame_threshold.copy()
h, w = frame_threshold.shape[:2]
mask = np.zeros((h+2, w+2), np.uint8)
cv.floodFill(im_floodfill, mask, (0, 0), 255)
im_floodfill_inv = cv.bitwise_not(im_floodfill)
mask = frame_threshold | im_floodfill_inv

# Apply morphological operations
kernel = np.ones((3, 3), np.uint8)
mask = cv.morphologyEx(mask, cv.MORPH_OPEN, kernel, iterations=2)
mask = cv.morphologyEx(mask, cv.MORPH_CLOSE, kernel, iterations=4)

# Find contours
contours, _ = cv.findContours(mask, cv.RETR_EXTERNAL, cv.CHAIN_APPROX_SIMPLE)

if contours:
    # Merge contours using convex hull
    hull = cv.convexHull(np.vstack(contours))

    # Create a mask for the shell
    shell_mask = np.zeros_like(frame)
    cv.drawContours(shell_mask, [hull], -1, (255, 255, 255), -1)

    # Create a white background
    white_background = np.ones_like(frame) * 255

    # Combine the shell with the white background
    result = np.where(shell_mask == 255, frame, white_background)
else:
    result = frame # If no contour is found, return the original image

# Save the processed image
cv.imwrite(output_path, result)

```

Figure A.6: Processing the images to remove the shadows.

### iii. Deep Learning

This section outlines the key steps in the deep learning pipeline, including the use of random undersampling to address class imbalance and data augmentation to increase variability in the dataset. The convolutional neural network (CNN) architecture consists of three convolutional layers, followed by a flatten layer and two dense layers. Additionally, early stopping was integrated to halt model training when the validation loss does not improve, and callbacks such as ReduceLROnPlateau were implemented as safeguards against overfitting. ModelCheckpoint was used to save the best model for each fold, allowing the final results to be revisited and analyzed after training; however, it was not heavily utilized in this study.

```

# Get male and female filenames
male_samples = sorted(os.listdir(male_folder))
female_samples = sorted(os.listdir(female_folder))

# Randomly sample 127 male samples to match female sample size
male_samples_to_keep = random.sample(male_samples, undersample_size)

# Copy the selected male samples to the balanced male directory
for file in male_samples_to_keep:
    shutil.copy(os.path.join(male_folder, file), os.path.join(balanced_male_dir, file))

# Copy all female samples to the balanced female directory (since it's already balanced)
for file in female_samples:
    shutil.copy(os.path.join(female_folder, file), os.path.join(balanced_female_dir, file))

```

Figure A.7: Random undersampling applied in deep learning to balance class distribution in the datasets.

```
def create_data_augmentation():
    return tf.keras.Sequential([
        layers.RandomFlip("horizontal"),
        layers.RandomRotation(0.05),
        layers.RandomZoom(0.05),
    ])
```

Figure A.8: On-the-fly data augmentation used to create a variety of random transformation to increase variation in the training images.

```
def create_cnn_model(img_width=256, img_height=256):
    model = Sequential([
        layers.Input(shape=(img_width, img_height, 3)),
        layers.Rescaling(1./255),
        layers.Conv2D(16, (3,3), activation='relu'),
        layers.MaxPooling2D(2,2),
        layers.Conv2D(32, (3,3), activation='relu'),
        layers.MaxPooling2D(2,2),
        layers.Conv2D(64, (3,3), activation='relu'),
        layers.MaxPooling2D(2,2),
        layers.Flatten(),
        layers.Dense(128, activation='relu'),
        layers.Dropout(0.5),
        layers.Dense(1, activation='sigmoid')
    ])
    return model
```

Figure A.9: CNN architecture used for training the image dataset.

```
history = model.fit(
    train_ds,
    epochs=no_epochs,
    validation_data=val_ds,
    verbose=1,
    callbacks=[
        EarlyStopping(monitor='val_loss', patience=8, restore_best_weights=True, verbose=1),
        ReduceLROnPlateau(monitor='val_loss', factor=0.5, patience=3, verbose=1),
        ModelCheckpoint(f'best_model_fold_{fold_no}.h5', monitor='val_loss', save_best_only=True, verbose=1)
    ]
)
```

Figure A.10: Early Stopping and ReduceLROnPlateau used as safeguard against overfitting.

## **Appendix B**

### **Resource Persons**

This section of the paper presents information about the resource persons who contributed to and assisted the researchers during the data gathering process.

#### **Dr. Victor Marco Emmanuel N. Ferriols**

Provided blood cockles samples used in this study

Director, University of the Philippines Institute of Aquaculture

[vnferriols@up.edu.ph](mailto:vnferriols@up.edu.ph)

#### **Ms. Allena Esther D. Arteta**

Performed spawning of blood cockles samples, assisted the researchers with dissection and sex identification.

Research Associate, Institute of Aquaculture

[adarteta@up.edu.ph](mailto:adarteta@up.edu.ph)

**Ms. LC May C. Gasit**

Performed spawning of blood cockles samples, assisted the researchers with the dissection and sex identification

Research Associate, Institute of Aquaculture

[lcgasit@up.edu.ph](mailto:lcgasit@up.edu.ph)

**Sheila G. Untalan**

Performed spawning of blood cockles samples, assisted the researchers with the dissection and sex identification

Research Associate, Institute of Aquaculture

**Joel M. Fabrigas**

Assisted the researchers with the dissection and sex identification

Hatchery Staff, Institute of Aquaculture

**Paul Andre M. Lopez**

Assisted the researchers with the dissection and sex identification

Hatchery Staff, Institute of Aquaculture

## Appendix C

# Data Gathering Documentation

This section of the paper presents the data gathering process, including spawning, dissection, sex identification, collection of linear measurements, and image capture from six different camera angles.



Figure C.1: Sex identification through spawning of *T. granosa*.



Figure C.2: Sex-based separation of *T. granosa* samples post-spawning.



Figure C.3: Sex identified female through dissection of *T. granosa*.

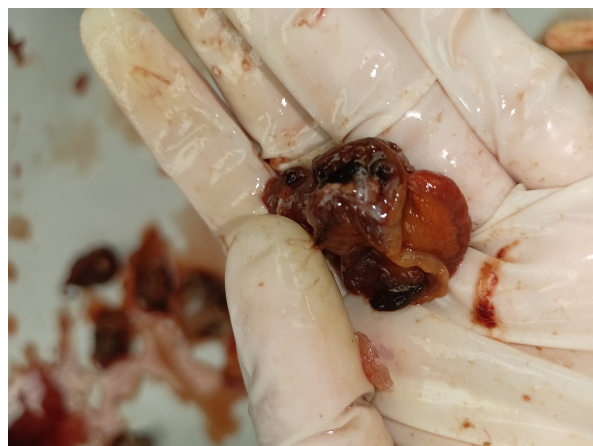


Figure C.4: Sex identified male through dissection of *T. granosa*.

Litob_Id	Length	Width	Height	Rib count	Length (Hinge Line)	Distance Umbos
10001	48.05	37.6	32.15	20	33.55	4.1
20001	48.05	37.6	32.15	20	33.55	4.1
30001	48.05	37.6	32.15	20	33.55	4.1
40001	48.05	37.6	32.15	20	33.55	4.1
50001	48.05	37.6	32.15	20	33.55	4.1
60001	48.05	37.6	32.15	20	33.55	4.1
10002	47.4	32.5	32.25	20	33.1	3.05
20002	47.4	32.5	32.25	20	33.1	3.05
30002	47.4	32.5	32.25	20	33.1	3.05
40002	47.4	32.5	32.25	20	33.1	3.05
50002	47.4	32.5	32.25	20	33.1	3.05
60002	47.4	32.5	32.25	20	33.1	3.05
10003	43.3	34.1	31.25	21	32.05	4.5
20003	43.3	34.1	31.25	21	32.05	4.5
30003	43.3	34.1	31.25	21	32.05	4.5
40003	43.3	34.1	31.25	21	32.05	4.5
50003	43.3	34.1	31.25	21	32.05	4.5
60003	43.3	34.1	31.25	21	32.05	4.5
10075	50.05	35.05	32.05	21	30.05	4.1
20075	50.05	35.05	32.05	21	30.05	4.1

Figure C.5: Linear measurements of female *T. granosa*.

Litob_Id	Length	Width	Height	Rib count	Length (Hinge Line)	Distance Umbos
110004	43.1	33.05	28.15	21	28.5	3.05
120004	43.1	33.05	28.15	21	28.5	3.05
130004	43.1	33.05	28.15	21	28.5	3.05
140004	43.1	33.05	28.15	21	28.5	3.05
150004	43.1	33.05	28.15	21	28.5	3.05
160004	43.1	33.05	28.15	21	28.5	3.05
110005	41.1	31.05	27.6	20	23.05	3.35
120005	41.1	31.05	27.6	20	23.05	3.35
130005	41.1	31.05	27.6	20	23.05	3.35
140005	41.1	31.05	27.6	20	23.05	3.35
150005	41.1	31.05	27.6	20	23.05	3.35
160005	41.1	31.05	27.6	20	23.05	3.35
110006	43.2	33.45	29.35	20	29.35	3.3
120006	43.2	33.45	29.35	20	29.35	3.3
130006	43.2	33.45	29.35	20	29.35	3.3
140006	43.2	33.45	29.35	20	29.35	3.3
150006	43.2	33.45	29.35	20	29.35	3.3
160006	43.2	33.45	29.35	20	29.35	3.3
110007	41.5	32.55	27.7	20	24.1	3.7
120007	41.5	32.55	27.7	20	24.1	3.7

Figure C.6: Linear measurements of male *T. granosa*.

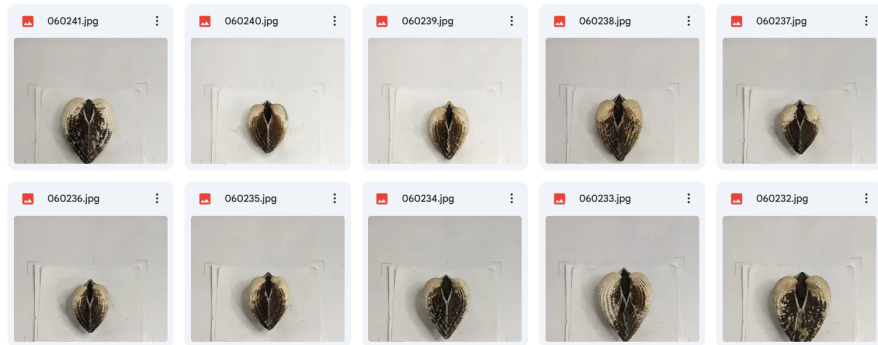


Figure C.7: Captured images of female *T. granosa*.

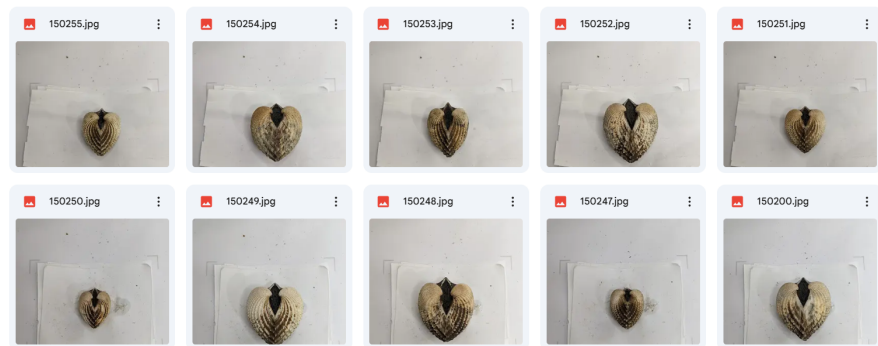


Figure C.8: Captured images of male *T. granosa*.